Copy No. 8

NASA PROGRAM APOLLO WORKING PAPER NO. 1193

PRELIMINARY WARNING CRITERIA FOR THE SOLAR PARTICLE ALERT NETWORK

NATIONAL AERONAUTICS AND SPACE ADMINISTRATION
MANNED SPACECRAFT CENTER
HOUSTON, TEXAS

January 28, 1966

NASA PROGRAM APOLLO WORKING PAPER NO. 1193

PRELIMINARY WARNING CRITERIA FOR THE SOLAR PARTICLE ALERT NETWORK

PREPARED BY

Manuel D. Lopez
Manuel D. Lopez
AST, Radiation and Fields Branch

Anna Lou Bragg
Anna Lou Bragg
AST, Radiation and Fields Branch

Jerry L. Modisette
Jerry L. Modisette
Chief, Radiation and Fields Branch

AUTHORIZED FOR DISTRIBUTION

Warren Gillespie, Jr.
for Maxime A. Faget
Assistant Director for Engineering and Development

NATIONAL AERONAUTICS AND SPACE ADMINISTRATION
MANNED SPACECRAFT CENTER
HOUSTON, TEXAS
January 28, 1966

CONTENTS

TABLES

FIGURES

PRELIMINARY WARNING CRITERIA FOR THE SOLAR PARTICLE ALERT NETWORK

By Manuel D. Lopez, Anna Lou Bragg, and Jerry L. Modisette

INTRODUCTION

The Solar Particle Alert Network (SPAN) is being developed to provide the Apollo program with warnings of impending solar flare particle events, including estimates of their severity, so that action can be taken to reduce the radiation dose received by the astronauts. SPAN consists of a network of solar radio and optical H_α telescopes located at terminals of the Apollo world-wide communications and tracking network. The telescopes are designed to observe phenomena associated with acceleration of energetic solar particles. By operating 24 hours a day and being integrated with the Apollo Mission Control Center, information on these phenomena can be rapidly transmitted to the flight director.

The objective of the warning criteria is to provide the means for interpreting SPAN observations. The criteria should incorporate RF and H_α data to determine if a particle event has occurred on the sun, if the particles will reach the earth, and what the particle flux will be. The analysis to develop the criteria was begun with certain preconceived ideas, which are summarized as follows:

1. Type IV μ (micro-wave) RF bursts are a result of synchrotron emission from electrons accelerated at the same time as the ions comprising a solar flare particle event.

2. Although type IV μ RF bursts are a positive indication of the acceleration of solar flare particles, the particles may not reach the earth either because of local trapping or because of the interplanetary magnetic field configuration.

3. The transport and/or trapping of solar particles is determined by solar surface activity, either during or for a few days preceding the acceleration of particles, for example, the transport of particles from the sun to the earth is governed by the coronal and interplanetary magnetic fields, which in turn are carried out from the solar surface by the solar wind.

With the above ideas in mind, the approach toward development of a warning criteria has been to use RF data to determine if and how many particles are accelerated at the sun, and then to use optical criteria to aid in determining whether the particles will reach the earth. Accordingly, the two criteria are discussed separately.

WARNING CRITERIA BASED ON RF TYPE IV μ BURSTS

The type IV μ RF bursts are considered to be synchrotron emission from electrons accelerated at the same time as the solar flare particles (ref. 1). Since the same process can account for the acceleration of both positive and negative particles, a quantitative correlation between the synchrotron radiation intensity and the number of positive particles eventually arriving at the earth would be expected. However, because of the other independent parameters affecting the escape and transport of the particles to the earth, such a correlation would have considerable scatter.

Several studies have been made of the particle flux-RF intensity correlations, including Webber (ref. 2), Fletcher et al (ref. 3), and Shlanta (ref. 4). Webber's correlation of 10 000 Mc/sec burst intensity with particle flux greater than 10 MeV is reproduced as fig. 1. Fletcher and Shlanta used a stepped criteria rather than the continuous rank correlation used by Webber, with similar results over a range of frequencies.

In this investigation a rank correlation is made in the frequency range covered by the SPAN telescopes (1420, 2695, and 4995 Mc/sec). It was pointed out by Fletcher and Shlanta that it is important to use original records rather than working with the onset time, duration, and peak flux data usually given in solar data compilations such as the IAU quarterly. This was verified by our own early attempts to correlate integrated RF intensities obtained by multiplying the peak flux by the duration. Therefore, Arthur E. Covington of the Ottawa Observatory of the Canadian National Research Council, and Dr. Haruo Tanaka of the University of Nagoya were approached regarding the use of their original records, to which they kindly consented.

An extensive event-by-event analysis was performed on the Ottawa data at 2800 Mc/sec. The 2800 Mc/sec data was initially surveyed to obtain all bursts having an integrated intensity of more than 10^{-18} joules - m^{-2} - $(c/s)^{-1}$ as determined by multiplication of peak flux by duration.

There were over 200 such bursts. The first problem was to determine which of these bursts were probably associated with the acceleration of solar flare particles. In a compilation by Jonah, Prince, and Hedeman (ref. 5) of solar and terrestrial phenomena, various observers recorded a total of 38 PCA events having onset times such that Ottawa could have observed an associated RF burst. Thirty-five of these events had associated RF bursts which were observed by Ottawa and one (November 20, 1960) was eliminated for reasons to be stated later. Of the two particle events with no associated RF bursts, one (August 29, 1959) had its associated flare $1\frac{1}{2}$ hours before sunrise at Ottawa, the other (November 4, 1957) was a small event with no logical RF or flare association. All of the 35 RF bursts with associated particle events had integrated RF intensities of at least 10^{-17} joules - m^{-2} - $(c/s)^{-1}$. It was, therefore, assumed that RF bursts having less energy either were not associated with particle acceleration, or that there were so few particles as to elude detection even if they reached the earth. These smaller bursts were dismissed from further consideration.

There remained a total of 85 bursts at 2800 Mc/sec intensities greater than 10^{-17} joules - m^{-2} - $(c/s)^{-1}$. The energies of these RF emissions were redetermined by integrating the intensity-time-curves. Table 1 is a list of these bursts, along with data on the associated solar flare particle events where such associations were found.

Using this simple criteria of a minimum integrated burst energy of 10^{-17} joules - m^{-2} - $(c/s)^{-1}$ there is a false alarm rate of 2.4 bursts per particle event, with one particle event out of 38 missed.

In order to obtain criteria for solar particle event sizes, the correlation of integrated RF burst energy with integrated particle flux was investigated. The PCA events were investigated in detail to ascertain the confidence to be placed in each PCA event-RF burst association.

As a result it was decided that the burst recorded on November 20, 1960, was probably not the burst associated with the particle event observed on the following date. The burst occurred from 2023 to 2105 UT. Sunset for Ottawa was at 2130 UT. At 2126, a second flare was observed, reaching a maximum at 2258 UT. Since the onset of particles was at 0200 UT November 21, either flare could have accounted for the event.

The importance of flare as given by various observatories are listed below:

	Flare onset	Imp.	Sec. flare onset	Imp.
McMath-Hulbert	2017	1	2126	2
Sac peak			2126	2
Climax	1955	3	2117	3
Honolulu			2132	1
Lockheed	2017	1	2114	1

The November 20, 1960 burst was omitted from the flux-intensity correlations, but was included as a false alarm in subsequent analyses. The August 31, 1956 event was eliminated from the flux-intensity correlation because the recorder went off scale during most of the burst and no reliable estimate of the integrated intensity could be made.

The five events in table 1 for which sunrise or sunset appears were eliminated from the flux density correlations because these events began well before sunrise or ended well after sunset. No accurate determination of the burst's peak intensity could be made. These bursts were not counted as false alarms.

Twenty-eight events remain for which adequate RF data were available. Two of these events, the May 4, 1960 and July 12, 1961 events were considered adequate for the analysis even though the RF emissions began before Ottawa's observing period. The IAU quarterly shows that maximums at other frequencies were reached at 1033 UT (9400 Mc/sec) and 1042 UT (1500 Mc/sec) for the May 4 event while maximums were reached at 1029 UT (9100 Mc/sec) and 1042 UT (1500 Mc/sec) for the July 12 event. It is believed that the Ottawa data recorded the major portion of each burst and, therefore, were included in the analysis.

Fifteen of the twenty-eight bursts could be associated with Webber's particle data (ref. 2). These bursts and corresponding PCA events form the core of the Ottawa RF energy-particle flux correlation. Table II lists these events along with pertinent optical information. Also included in table II are four events for which rough estimates of particle event sizes were made from Bailey's forward scatter data reported in reference 6 by Modisette, Vinson, and Hardy, and one event calculated from data in reference 7. Ten MeV integrated particle fluxes had been estimated by multiplication of peak flux intensity and duration. An extrapolation from 10 MeV to 30 MeV was made assuming the average rigidity fit for a model particle event.

Figure 2 shows the particle flux-RF energy correlation for Webber's data alone while figure 3 shows for comparison the combination of Webber

and estimated 30 MeV particle fluxes from forward scatter. It was decided that the various extrapolations in getting the forward scatter data into the same form as Webber's data had introduced errors in the event size estimates, so that only Webber's 15 events were used for subsequent analyses. It can be seen from figure 2 that a fair amount of scatter remains. It was felt that much of the scatter could be attributed to variations in the background RF radiation. In an attempt to treat this problem, correlations were made using the integrated RF intensity above a fixed level for all events and with integrated intensity above 0.1 and 0.2 of the peak. Figure 4 shows a RF burst at 2800 Mc/sec with the various baselines drawn in. Figure 5, 6, 7, respectively, are the correlations for integrated intensities above a fixed level of 50×10^{-22} watts - m^{-2} - $(c/s)^{-1}$ over the quiet sun, and 10 percent and and 20 percent of the peak RF flux intensity. Reduction in scatter is not so obvious from the figures, but the correlation coefficients reflect the improvement. The best correlation is obtained using 0.2 times the peak intensity as a base line although the difference between the correlation and that using a base line of 0.1 times the peak is not statistically significant.

A number of other correlations were investigated using Webber's particle event data, including peak intensity (fig. 8), duration of burst (fig. 9), and integrated intensity divided by duration (fig. 10). All of these parameters show significant correlations with the integrated particle flux, but none are as good as the integrated burst intensities.

The results of the analysis on the 2800 Mc/sec data show that the integrated intensity of RF type IV μ burst above a suitable baseline is useful as an indicator of the integrated particle flux during a solar flare particle event. It remains for further analysis and additional data to reduce the false alarm rate.

The Nagoya data were checked to ascertain if an equivalent correlation existed for 3750 Mc/sec. There are no known particle events missed by Nagoya. Table III lists the PCA events and RF bursts considered. The particle events for which an associated RF burst occurred during sunrise or sunset were eliminated from the correlation. Using the integrated intensity above 0.1 times the peak value, the correlation shown in figure 11 is obtained. Considerably more scatter exists for the 3750 Mc/sec correlation than for the 2800 Mc/sec correlation. It is not known at this time whether this scatter is real.

It should be pointed out that the analysis of the Ottawa data leans rather heavily on the initial assumption that there exists a relationship between the acceleration of particles and the RF bursts. Therefore, considerably more freedom was exercised in the elimination of data to

reduce scatter than would have been reasonable had the object been to establish the existence of a relationship.

OPTICAL CRITERIA

Introduction

The discussion of the optical criteria really concerns a combined criteria, since the objective of the optical criteria is to improve the RF predictions. There is also some additional development of the RF analysis in this section. The philosophy outlined in the introduction leads to the idea that the optical criteria should introduce factors governing the transport of particles from the sun to the earth. It is generally agreed that the coronal and interplanetary magnetic field configuration, together with the boundary condition of the location of the origin of the particles, determine where the particles go and in what numbers. The origin of the particles is determined by the location of the associated flare. Since the equations of magnetohydrodynamics are reasonably well established, one might think that spectroscopically determined values of the bulk properties of the base of the corona would allow the calculation of the characteristics of the interplanetary medium. Such an approach has had only limited success thus far, for example, no analysis has included the effects of magnetic forces or solar rotation on the solar wind, and there remains some question as to the energy source of the solar wind. For this reason a discussion of the physical reasoning behind the selection of certain optical parameters for detailed analysis must proceed with a certain amount of "hand-waving." However, the physical reasoning is very important, because the abundance of parameters and the sparseness of data points makes it relatively easy for a glib statistician to find a plausible set of correlations based on fortuitous circumstances.

There are, of course, several things that can be said with assurance about the processes governing the transport of charged particles from the sun to the earth. The spiral interplanetary field may be regarded as well established, although a detailed understanding of the occurrence of irregularities is lacking. It may be further stated with some assurance that this spiral field will make it easier for the particles to arrive at the earth from the west limb of the sun, and indeed, data on the distribution in longitude of particle-producing flares confirm this prediction (figs. 12 and 13).

It is apparent, however, that properties of the interplanetary magnetic field other than its spiral configuration influence the transport of solar flare particles, since there are many events, including some large ones, originating on the east limb. Somehow, the particles are

crossing the field lines. Since the collision frequency of the particles is so low that we would normally expect the "frozen in flux" assumption to hold, we are led to the conclusion that the particles are scattering from magnetic irregularities. Therefore, we are interested in observable parameters related to the distribution of these scattering centers.

There are small-scale irregularities in the interplanetary field when it is carried past the earth. Since the field is frozen into the plasma, and since the solar wind undergoes a large radial expansion in leaving the corona (much larger than the lateral expansion) one would expect these irregularities to be larger close to the sun, that is, if we moved an element of the solar wind back towards the sun, the radial compression would amplify the transverse component of the field. The picture is complicated by our ignorance of the level in the corona at which these irregularities are generated and of the distribution of solar wind velocity with radial distance. In general, however, we may say that anything that slows the solar wind should increase the concentration of scattering centers.

In reference 8, James reports the results of solar radar studies which appear to show a slowing down of the solar wind above large active centers. This is a rather unexpected result, since the solar wind undergoes a large acceleration between the sun and the earth, and one would not expect a slowing down in between. It is possible to devise magnetic forces which could produce this result, since if the transverse component of the field falls off more slowly than $1/r$, the net force will be directed inward. The idea that magnetic forces may be important introduces the plages as important observable features, since the plage marks the extent of strong solar fields. The plage also appears to be an important indicator of an active or potentially active solar region. Another factor that may make plages important is that once the region of slowing down (0.5 - 1.0 radii above the photosphere) is passed, the generally stronger magnetic and particle pressures above a plage may cause it to expand laterally at the expense of surrounding regions, facilitating the spread in longitude of particles from the region of the plage even if they stay on their field lines.

Other features of the sun indicating magnetic activity include the sunspots and their magnetic classification. An optical criteria should include the flare importance, since the correlation with particle event size is well established. The flare importance is probably somewhat redundant to the RF intensity, being a measure of the number of particles accelerated, but one might also argue that a large flare would spread its particles over a larger area in the chromosphere, giving them a head start towards a wide spread in longitude.

PARAMETERS SELECTED

It is desirable to limit the number of parameters studied, both to avoid statistical difficulties and to allow the investigators to assess the data more critically. On the basis of the above considerations, longitude, plage area, plage brightness, flare importance, sunspot area, sunspot magnetic classification, sunspot Zurich type, and plage clustering were selected for study. This data was obtained from several sources (refs. 5, 9, 10, and 11) for three sets of data: the 42 particle events given by Webber, and the RF bursts from Ottawa and Nagoya. It was also decided to investigate the variation of false alarm rate with event size for the RF data to check out the effect reported by Fletcher et. al. (ref. 3).

After a preliminary examination of the data, it was decided to omit Zurich type and magnetic classification of the sunspots from further consideration. Although the particle events consistently showed E, F, or H type sunspots and γ or $\beta\gamma$ magnetic classifications, the trends with event size were much less apparent than for the other parameters, and the RF studies reported below indicate the importance of variations of event size. Clustering of plages may be as important as a large plage. Proper consideration of this effect would require careful definition of "clustering", but it is intended to investigate this parameter more thoroughly in the future.

LONGITUDE EFFECT

A dependence of the production of solar flare particle events upon heliographic longitude has been recognized for some time, and is consistent with our present understanding of the interplanetary magnetic field. Figures 12 and 13 show the distribution in longitude of the flares producing particle events for several compilations of data. All show a preponderance of west limb events. An obvious use of this effect would be to reduce the false alarm rate for west limb events, and to increase the false alarm rate for east limb events. The operational significance of this effect would be to permit a more careful assessment of the confidence levels to be placed on the individual SPAN warnings. The overall false alarm rate is not changed by this effect.

In accordance with our idea of spreading in longitude due to diffusion or scattering of particles, the source of the particles is of obvious importance. The particle flux should be a function of the separation in longitude of the flare and the field line connecting the earth to

the sun. The form of the function probably varies, however. In particular, one might expect a difference between events predominantly of a diffusive nature and events for which the particles come directly down the field lines. To look for the difference, one must first determine which events fall into each category. The best parameter to differentiate these events that is available for a large number of events is probably the delay time, between flare or RF maximum and particle onset. In figures 14 to 17 the events are divided into groups having delay times greater and less than 1, 2, 3, and 4 hours. It is apparent that the longitudinal asymmetry comes from the events with short delay times. This analysis is based on data which would not be available for warning criteria, so that it is necessary to relate diffusive and "straight-on" events by some observable feature of the sun. An attempt to correlate plage area with delay time resulted in a large amount of scatter. The further exploitation of the longitude effect will be the subject of future development of the warning criteria.

PLAGE EFFECTS

From the tabulated data, the effect of plage area is apparent. Plage brightness is somewhat less apparent, although the trend of brighter plages with larger events can be seen. The scatter indicates that a combination of plage parameters with other effects will be necessary, and that correlations obtained from analyzing the plage data alone would have very low confidence levels.

RF CRITERIA ALONE

The Ottawa RF false alarm rates for various event sizes were determined from the least square fit of figure 6. The table below shows the RF energy thresholds for prediction of the various event sizes.

RF energy	Predicted event size
$>1000 \times 10^{-18}$ J/m^2-cps	$>10^9$
>270	$>10^8$
>78	$>10^7$
>22	$>10^6$
>10	$>10^5$

Using the above thresholds and data from table I, false alarm rates were determined.

The following are comments about the makeup of the false alarm table. The number of actual events in the 10^6 and larger columns consider only Webber particle fluxes. Events for which no estimates of particle fluxes are given were included in the 10^5 column. Particle events with associated bursts occurring during sunset or sunrise were also included in the 10^5 column. The two events for which no RF was detected were not included in the false alarm table.

The following table gives information on false alarms for 2800 Mc/sec using least square fit RF thresholds:

Event size	$>10^5$	$>10^6$	$>10^7$	$>10^8$	$>10^9$
RF bursts	85	52	19	5	0
Actual events	35	13	6	3	1
False alarm rate	2.4/1	4/1	3.2/1	1.7/1	?

A decrease in false alarms is indicated as the burst size increases. This may be a real effect even though the number of large bursts on which to base this is rather small.

Many of the events in the previous discussion were underestimated. Hence an RF-particle flux criteria was developed from an envelope curve (fig. 18) parallel to the least square fit in figure 6. No events were underestimated with this curve. The following false alarm table resulted.

Event size	$>10^5$	$>10^6$	$>10^7$	$>10^8$	$>10^9$
RF bursts	85	85	31	10	4
Actual events	35	13	6	3	1
False alarm rate	2.4/1	6.5/1	5/1	3.3/1	4/1

The decrease in false alarm rate with larger events is no longer obvious, in view of large number of bursts corresponding to $>10^9$ particles. However, if we note that one of the $>10^8$ events is listed by Webber as 9.6×10^8, and another as 9.1×10^8, it appears that there may

be something to the effect. All the above discussion is based on the Ottawa data. For the Nagoya data, using the envelope line (fig. 19), the results are as follows:

Event size	$>10^5$	$>10^6$	$>10^7$	$>10^8$	$>10^9$
RF burst	87	80	37	16	10
Actual events	25	15	11	6	3
False alarm rate	3.5/1	5.2/1	3.4/1	2.7/1	3.3/1

Again, there are some 10^8 events that are almost 10^9, pointing out a disadvantage of this stepwise criteria.

It is of some interest at this point to comment on the envelope lines for the RF data. Although the least-square fits of the Nagoya and Ottawa data are quite different, the envelope lines are almost the same. This supports the idea that the RF burst is an absolute measure of the number of particles accelerated, while various other factors reduce the number of particles eventually reaching the earth.

COMBINED CRITERIA

Using the 42 events for which Webber gives size estimates, and the Ottawa and Nagoya RF data, it is possible to determine minimum values of the RF flux (from envelope), Plage area, Plage brightness, Flare importance, and Sunspot area associated with each decade of event size. These values are tabulated below:

Event size	3750 Mc/sec RF burst	2800 Mc/sec RF burst	Plage area	Plage brightness	Flare importance	Sunspot area
$>10^9$	270	500	8000	3	3	1400
$>10^8$	76	140	5000	3	3	550
$>10^7$	21	38	4000	3	2+	500
$>10^6$	10	10	3000	2.5	1(3E)	___
$>10^5$	10	10	2000	2.5	1	___

The (3E) under flare importance for $>10^6$ indicates that a flare must be at least of importance 3 on the east limb.

Using the combined criteria on the Ottawa RF bursts, and the optical parameters given in table VII, we obtain the following results:

Event size	$>10^5$	$>10^6$	$>10^7$	$>10^8$	$>10^9$
Predicted	68	45	16	7	2
Actual	35	13	6	3	1
False alarm rate	1.95/1	3.5/1	2.7/1	2.3/1	2/1

Again, the 10^9 false alarm was a 9.1×10^8 event and two 10^8 false alarms were 5×10^7 and 7×10^7 events.

Using the Nagoya data, table VI, and the combined criteria we obtain the following results:

Event size	$>10^5$	$>10^6$	$>10^7$	$>10^8$	$>10^9$
Predicted	54	40	20	7	4
Actual	25	15	9	6	3
False alarm rate	2.2/1	2.7/1	2.2/1	1.2/1	1.3/1

In this case the $>10^9$ false alarm was a 7.2×10^8 event and the 10^8 false alarm was a 7.2×10^7 event. The combined criteria has reduced the Nagoya RF false alarms considerably. It is encouraging that with the combined RF and optical criteria that the false alarm rates for Ottawa and Nagoya are approximately equal.

CONCLUSION

It has been shown in this paper that there is a relationship between solar μ RF burst energies and integrated solar flare particle fluxes. Definite correlations between 2800 Mc/sec RF bursts and integrated flux greater than 30 MeV exists while 3750 Mc/sec shows a weaker dependence. Since an envelope curve was found to fit both Ottawa and Nagoya data, it

was argued that a number of independent factors influence the total number of particles arriving at the earth. However, the same envelope curve was shown to fit both the Nagoya and the Ottawa data, supporting the interpretation that the RF burst integrated intensity in a direct measure of the acceleration of particles, with other factors determining the transport of the particles to the earth.

Particle events greater than 10^8 are of most concern to the Apollo mission. Hence with an Ottawa RF criteria (detection of a burst with energy greater than 140×10^{-18} joules - m^{-2} - cps) signaling the occurrence of a PCA and predicting a particle flux $>10^8$ will have a false alarm rate of 3.3 to 1, when observable optical parameters are included in the criteria the false alarm rate drops to 2.3 to 1. The Nagoya RF criteria has a 2.7 to 1 false alarm rate for prediction of $>10^8$ particles events and a 1.2 to 1 false alarm rate for the combined optical and RF criteria.

The longitude effect has only been considered in a limited sense in developing the optical criteria and has not been investigated in any detail. It has been shown that events with onset <3 hours may be considered as direct events with a western longitudinal predominance, and those events >3 hours as diffusive events with no longitudinal dependence. Knowledge of particle events being either diffusive or direct would aid in eliminating false alarms on eastern longitudes plus give an indication of the probable time of particle onset.

The warning criteria based on combined RF and optical data show substantial decreases in the false alarm rates over the RF criteria alone. The remaining false alarms are largely due to the constraint imposed on the criteria that no events should be underestimated, and to the use of stepped criteria. This result shows that the next step in the warning criteria development is to apply multiparameter correlation analysis to the parameters shown to be important, to obtain continuous functions which estimate the average event size for a given set of conditions, rather than the maximum as was done in the current analysis. The resulting criteria will be more amenable to confidence analysis, and to extrapolation to larger events.

REFERENCES

1. Wild, J. P.: Journal of the Physical Society of Japan 17. Supplement A-II, 249, 1962.

2. Webber, W. R.: An Evaluation of the Radiation Hazard Due to Solar Particle Events. Boeing Report D2-90469, Dec. 1963.

3. Fletcher, J. D.: Solar Radio Emission as Criteria for Solar Proton Event Warning. AIAA Journal, Dec. 1964.

4. Shalanta, A.: An Analysis of the Relation Between Solar Radio Emission and Large Solar Cosmic Ray Increases. Schellenger Research Laboratories Report on NASA grant NGR 44-020-001, June 1965.

5. Jonah, F. C.; Prince, H. Dodson; and Hedeman, E. R.: Solar Activity Catalogue. Ling-Temco-Vought reports on NASA contract NAS9-2469, 1965.

6. Modisette, J. L.; Vinson, T. M.; and Hardy, A. C.: Model Solar Proton Environments for Manned Spacecraft Design. NASA TN D-2746, April 1965.

7. Bailey, D. K.: Journal of the Physical Society of Japan 17. Supplement A-I, Part I, Jan. 1962.

8. James, Jesse C: Radar Echoes from the Sun. IEEE Transactions on Military Electronics. Volume MIL-8, Nov. 3 and 4, July-October 1964.

9. McMath-Hulbert Working List of Flares

10. IAU Quarterly

11. CRPL Monthly Bulletin of Solar Activity

TABLE I.- COMPILATION OF OTTAWA (2800 Mc/sec) RF BURST PARAMETERS AND ASSOCIATED SOLAR AND TERRESTIAL PHENOMENA FOR THE PERIOD 1955 TO 1961

Date	RF burst, UT		RF peak intensity, 10^{-22} W/m^2-cps	RF burst energy above 10 percent of peak, 10^{-18} J/m^2-cps	Particle onset time, UT	PCA observers (a)	Particle event size, P > 30 MeV	Flare-			
	Start	Max.						Location	Imp.	Start, UT	Max., UT
June 18, 1955	1907	1908	1 575	43				S22 W21	3	1905	1910
July 9, 1955	1906	1922	309	30				No data			
Feb. 16, 1956	1757	1813	650	60				N20 E08	2+	1805	
Feb. 19, 1956	1427	1435	650	29				N25 W23	1+	1430	1445
Mar. 13, 1956	1452	1454	850	14				N21 E50	2	1453	
Mar. 15, 1956	1622	1627	1 300	43				N22 E21	2+	1625	1635
June 20, 1956	1938	1939	340	12				No data			
Aug. 31, 1956	1231		>340 Off scale	>61	1430	B	2.5×10^7	N16 E16	3	1226	1243
Sep. 17, 1956	1940	1947	320	13				S20 W17	2+	1942	1950
Nov. 13, 1956	1433	1440	180	13	2000	B		N16 W10	2	1430	1501
Dec. 26, 1956	1403	1454	915	132				S17 W11	2	1401	1412
Jan. 6, 1957	1758	1827	585	42				N16 W53	1-	1822	
Apr. 12, 1957	1855	1900	525	12				S25 W73	2	1850	1920
Apr. 14, 1957	1700	1915	37	40				S23 W28	1	1708	
Apr. 16, 1957	1043	1050	1 650	87				N30 E85	3	1040	1105
Apr. 17, 1957	2006	2042	6 000	546				N20 E69	3+	2000	2116
June 3, 1957	1042	1051	290	17				S18 W18	3	1040	
June 19, 1957	1608	1610	2 325	34		B		N20 E45	2	1609	1613
July 15, 1957	2019	2043	300	12				No logical flare association			
July 16, 1957	1741	1756	350	23				S33 W28	1+	1742	1804
July 20, 1957	1735	1750	145	14				No logical flare association			
July 24, 1957	1759	1838	1 100	94	2015	L,H		S24 W27	3	1801	1828
Aug. 1, 1957	1400	1815	25	22				S35 E04	1	1352	1420
Aug. 9, 1957	1304	1517	40	27	1600	B	1.5×10^6	S33 W77	1	1330	1355
Aug. 28, 1957	2017	2019	760	10	0000(8/29)	B,H		S28 E30	2+	2010	2024
Aug. 29, 1957	No burst recorded				1400	B,L,H		S25 E20	2	1031	1052
Aug. 31, 1957	1300	1321	3 900	350	1500	B		N25 W02	3	1257	1312
Sep. 2, 1957	1300	1324	120	30	1700	B		S34 W36	2+	1313	1316
Sep. 3, 1957	1417	1426	1 350	51				N23 W30	3	1412	1428
Sep. 18, 1957	1821	1825	275	47				N20 E02	3+	1815	1840
Sep. 21, 1957	1330	1337	790	49	1700	B	1.5×10^6	N10 W00	3	1330	1335

[a]List of PCA observers: B = Bailey, L = Leinbach, H = Hakura & Goh

TABLE I.- COMPILATION OF OTTAWA (2800 Mc/sec) RF BURST PARAMETERS AND ASSOCIATED SOLAR AND TERRESTIAL PHENOMENA FOR THE PERIOD 1955 TO 1961 - Continued

Date	RF burst, UT		RF peak intensity, 10^{-22} w/m^2-cps	RF burst energy above 10 percent of peak, 10^{-18} j/m^2-cps	Particle onset time, UT	PCA observers (a)	Particle event size, P > 30 MeV	Flare-				
	Start	Max.						Location		Imp.	Start, UT	Max., UT
Sep. 26, 1957	1915	1945	110	25	2100	B,L		N22	E15	3	1907	1957
Oct. 20, 1957	1640	1651	4 000	209	2100	B	5.0×10^7	S26	W35	3+	1644	1647
Nov. 4, 1957	No burst recorded				0200	B	9.0×10^6	No logical flare association				
Jan. 15, 1958	1640	1643	1 350	21				S13	W58	2+	1640	1642
Feb. 9, 1958	2105	?		Sunset	0600(2/10)	B,L,H		S12	W14	2+	2108	2142
Mar. 23, 1958	<1115			Sunrise	1500	B	2.5×10^8	S14	E78	3+	0947	1445
June 5, 1958	1614	1623	387	35				S18	E69	2+	1615	1631
June 28, 1958	1500	1745	23	32				S26	W20	1-	1434	
July 7, 1958	0027	?	875 at 0028	Sunset	0330	B,L,H,K	2.5×10^8	N25	W08	3+	0020	0110
July 30, 1958	1525	1529	400	15				S13	W64	2	1523	1530
Aug. 2, 1958	1840	1842	2 050	26				S14	W90	1-	1840	1841
Aug. 22, 1958	1430	1506	1 500	192	1530	B	7.0×10^7	N18	W10	3	1428	1450
Oct. 24, 1958	1439	1511	185	18				S05	W57	2+	1432	1457
Dec. 11, 1958	1805	1810	1 225	14				S02	E00	2	1802	1812
Dec. 12, 1958	1257	1301	1 500	20				S03	W08	2+	1229	1304
Jan. 21, 1959	1702	1708	600	12				N10	E48	3	1700	1709
Jan. 24, 1959	1450	1535	60	12				N12	W20	1	1454	1457
								S06	E20		1452	1453
Jan. 25, 1959	1410	1412	325	50				N18	W50	2	1406	1414
Feb. 9, 1959	1308	1317	160	10				N09	E87	2+	1230	
Mar. 22, 1959	1340	1345	525	12				N29	W50	1+	1338	1348
Apr. 7, 1959	1350	1450	51	26				N10	E84	2	1355	
May 8, 1959	2254	2257	2 220	29				N21	E83	2+	2252	2257
May 10, 1959	2100	2154	2 550	811	0030(5/11)	B,L,K	9.6×10^8	N18	E47	3+	2102	2140
May 11, 1959	2010	2021	900	75				N10	E41	3	2006	2030
June 9, 1959	1645	1740	1 800	146				N17	E90	2	1707	
June 18, 1959	1139	1140	1 225	14				N16	W12	3+	1130	1145
July 9, 1959	2043	2046	520	15				N18	E67	2	1930	1957
July 9, 1959	2112	2128	520	30				N19	E48	2	2115	2130
July 16, 1959	2118	2154	5 500	732	0000(7/17)	B	9.1×10^8	N16	W31	3+	2114	2132
Aug. 18, 1959	<1200	?	30 at 1200	Sunrise	1130	B	1.8×10^6	N12	W33	3	1014	1030

[a]List of PCA observers: B = Bailey; L = Leinbach; K = Kiruna; H = Hakura & Goh

TABLE I.- COMPILATION OF OTTAWA (2800 Mc/sec) RF BURST PARAMETERS AND ASSOCIATED SOLAR AND TERRESTIAL PHENOMENA FOR THE PERIOD 1955 TO 1961 - Concluded

Date	RF burst, UT		RF peak intensity, 10^{-22} w/m^2-cps	RF burst energy above 10 percent of peak, 10^{-18} j/m^2-cps	Particle onset time, UT	PCA observers (a)	Particle event size, P > 30 MeV	Flare-			
	Start	Max.						Location	Imp.	Start, UT	Max., UT
Aug. 31, 1959	1858	1906	270	10				N10 E11	1+	1850	1910
Dec. 2, 1959	1246	1248	875	11				N07 W16	2+	1219	
Dec. 4, 1959	1815	1910	40	16				N06 W44	2+	1814	1823
Jan. 11, 1960	2056	2108	220	13	0300 (1/12)	B,G,VA	4.0×10^5	N22 E03	3	2040	2126
Jan. 15, 1960	1340	1357	700	117	0300 (1/16)	G		S20 W68	2	1334	
Mar. 28, 1960	2048	2118	1 150E	127				N14 E37	2	2042	2056
Mar. 30, 1960	1518	1556	1 750	160	0300 (3/31)	L,K		N12 E11	2	1455	1540
Apr. 3, 1960	1745	2122	75	18				No logical flare association			
May 4, 1960	<1025	1046	600	69	1030	B,L,K,G,VA	6.0×10^6	N13 W90	3	1000	1016
May 6, 1960	1406	1434	695	69	1800	B,L,K,G,VA	4.0×10^6	S09 E07	3+	1404	1440
June 1, 1960	<1045	?	25 at 1045	Sunrise	≤1021	G,VA	4.0×10^5	N29 E46	3+	0823	0900
June 25, 1960	1148	1209	425	46	1700	G,D		N21 E06	3	1136	1215
June 27, 1960	2140	2158	140	17	23??	G		N22 W27	3	2140	2156
Aug. 11, 1960	1923	1928	1 100	26	00??	G,VA	6.0×10^5	N22 E26	2+	1916	1929
Sep. 16, 1960	1702	1756	2 000	185				S22 E67	1	1706	1724
Oct. 23, 1960	2056	2122	320	22				N22 E90	1+	2114	2130
Nov. 6, 1960	1628	1837	56	20				N13 E07	3	1752	1841
Nov. 12, 1960	1320	1346	5 500	606	1400	B,L,G,VA	1.3×10^9	N27 W04	3+	1315	1330
Nov. 20, 1960	2023	2027	400	25				N25 W90	1	2017	2020
									2	2126	2258
Dec. 5, 1960	1828	1838	330	23	05?? (12/6)	G		N26 E74	3+	1825	1838
July 11, 1961	1604	1745	1 500	138	0000 (7/12)	L	3.0×10^6	S07 E32	3	1615	1700
July 12, 1961	<1102	1113	1 200	88	1300	B,L	4.0×10^7	S07 E23	3	1000	1025
July 15, 1961	1510	1610	111	36	1545	L		S07 W20	2	1508	1512
July 20, 1961	1552	1621	1 800	94	0300 (7/21)	L	5.0×10^6	S06 W90	3	1553	1635
Sep. 10, 1961	1930	2001	900	95	2100	B,L,N		N08 W80	1	1958	2010
Sep. 28, 1961	2211	2218	800	36	2330	B,L,N	6.0×10^6	N13 E29	3	2202	2223

[a]List of PCA observers: B = Bailey; G = Gregory, VA = Van Allen; L = Leinbach; K = Karuna; N = NASA; and D = Dvoryashin

TABLE II.- LIST OF 20 OTTAWA (2800 Mc/sec) RF BURST AND ASSOCIATED PHENOMENA

WHICH CAN BE ASSOCIATED WITH WEBBER AND FORWARD SCATTER PARTICLE FLUXES >30 MeV

Date	RF burst, UT		RF peak intensity, 10^{-22} W/m^2-cps	RF burst energy integrated above, 10^{-18} J/m^2-cps			Particle event size, P > 30 MeV	Flare location		Flare imp.	Particle onset, UT	Flare time, UT	
	Start	Max.		Quiet sun	10 percent peak	20 percent peak						Start,	Max.,
Nov. 13, 1956	1433	1440	180	19	13	7	[a]1.2×10^8	N16	W10	2	2000	1430	1501
Aug. 9, 1957	1304	1517	40	36	27	19	1.5×10^6	S33	W77	1	1600	1330	
Aug. 28, 1957	2017	2019	760	12	5	4	[a]1.7×10^7	S28	E30	2+	2400	2010	2024
Aug. 31, 1957	1300	1321	3900	410	350	263	[a]5.3×10^7	N25	W02	3	1500	1257	1312
Sep. 2, 1957	1300	1324	120	45	30	19	[a]1.4×10^7	S34	W36	2+	1700	1313	1316
Sep. 21, 1957	1330	1337	790	20	13	9	1.5×10^6	N10	W06	3	1700	1330	1335
Oct. 20, 1957	1644	1651	4000	311	209	170	5.0×10^7	S26	W35	3+	2100	1644	1647
Aug. 22, 1958	1430	1506	1500	319	192	140	7.0×10^7	N18	W10	3	1530	1428	1450
May 10, 1959	2100	2154	2500	1048	811	630	9.6×10^8	N18	E47	3+	2430	2102	2140
July 16, 1959	2118	2154	5500	1040	732	535	9.1×10^8	N16	W31	3+	2400	2114	2132
Jan. 11, 1960	2056	2108	220	27	13	9	4.0×10^5	N22	E02	3	0300 (1/12)	2040	2126
May 4, 1960	<1025	1046	600	92	70	53	6.0×10^6	N13	W90	3	1030	1000	1016
May 6, 1960	1406	1434	695	146	69	46	4.0×10^6	S08	E07	3+	1800	1404	1440
Aug. 11, 1960	1916	1928	1100	36	26	19	6.0×10^5	N22	E26	2+	2400	1916	1929
Nov. 12, 1960	1320	1345	5500	866	606	470	1.3×10^9	N27	W04	3+	1400	1315	1330
July 11, 1961	1604	1745	1500	242	138	90	3.0×10^6	S07	E32	3	2400	1615	1700
July 12, 1961	<1102	1113	1200	120	90	70	4.0×10^7	S07	E23	3	1300	1000	1025
July 20, 1961	1552	1621	1800	187	94	70	5.0×10^6	S06	W90	3	0500 (7/21)	1553	1635
Sep. 28, 1961	2211	2218	800	52	36	25	6.0×10^5	N13	E29	3	2330	2202	2223
Sep. 10, 1961	1930	2001	900	120	95	78	[a]3.7×10^7	N08	W80	1	2100	1958	2010

[a]Estimated from forward scatter.

TABLE III.- COMPILATION OF NAGOYA (3750 Mc/sec) RF BURSTS AND ASSOCIATED PHENOMENA

WHICH CAN BE ASSOCIATED WITH WEBBER AND FORWARD SCATTER PARTICLE FLUXES >30 MeV

Date	RF burst, UT		RF peak intensity, 10^{-22} W/m^2-cps	RF burst energy integrated above, 10^{-18} J/m^2-cps			Particle event size, P > 30 MeV	Flare location		Flare imp.	Particle onset, UT	Flare time, UT	
	Start	Max.		Quiet sun	10 percent peak	20 percent peak						Start	Max.
Feb. 23, 1956	0334	0336	18 000	670	448	262	1.0×10^9	N23	W80	3	0400	0331	
Mar. 10, 1956	0447	0518	1 000	154	118	88	[a]1.1×10^8	N16	E88	2	0900	0515	
July 3, 1957	0727	0742	337	52	32	21	2.0×10^7	N14	W40	3+	1000	0712	0745
	0832	0843	763					N10	W42	3+		0830	0840
July 7, 1958	0027	0028	990	250	156	102	2.5×10^8	N25	W08	3+	0330	0020	0110
	0102	0111	1 700										
Aug. 16, 1958	0433	0439	5 800		300	160	4.0×10^7	S14	W50	3+	0600	0433	0440
Aug. 26, 1958	0005	0041	5 050	700	550	420	1.1×10^8	N20	W54	3	0330	0005	0027
Sep. 22, 1958			Sunset				6.0×10^6	S19	W42	2	1400	0738	0750
May 10, 1959	<2200		Sunrise				9.6×10^8	N18	E47	3+	0030	2102	2140
July 10, 1959	0200	0224	6 300	690	515	378	1.0×10^9	N20	E60	3+	0700	0206	0230
July 14, 1959	0330	0356	6 000	655	400	250	1.3×10^9	N17	E04	3+	0730	0325	0349
July 16, 1959			Sunrise				9.1×10^8	N16	W31	3+	0000	2114	2132
Apr. 5, 1960	0140	0202	6 000	820	510	340	1.1×10^6	N12	W63	2	0700	0215	0245
Apr. 28, 1960	0116	0130	260	28	17	12	5.0×10^6	S05	E34	3	0230	0130	0137
Apr. 29, 1960	0139	0140	115	67	51	38	7.0×10^6	N14	W21	2+	0500	0107	0210
	0356	0400	365										0400
May 13, 1960	0517	0532	3 750	635	500	386	4.0×10^6	N30	W67	3	0730	0519	0532
Sep. 3, 1960	0039	0105	12 000	227	160	111	3.5×10^7	N18	E88	2+	0500	0037	0108
Sep. 26, 1960	0525	0539	1 680	148	108	85	2.0×10^6	S22	W64	1+	1328	0525	0537
Nov. 15, 1960	0219	0222	11 600	1170	780	510	7.2×10^8	N25	W35	3	0430	0207	0221
Sep. 28, 1961	2212	2217	1 690	77	48	31	6.0×10^6	N13	E29	3	2330	2202	2223

[a]Estimated from forward scatter.

TABLE IV.- COMPILATION OF NAGOYA (3750 Mc/sec) RF BURST PARAMETERS AND ASSOCIATED SOLAR AND TERRESTIAL PHENOMENA FOR THE PERIOD 1956 TO 1961

Date	RF burst, UT		RF peak intensity, 10^{-22} W/m^2-cps	RF burst energy above 10 percent of peak, 10^{-18} J/m^2-cps	Particle onset time, UT	PCA observers (a)	Particle event size, P > 30 MeV	Flare-			
	Start	Max.						Location	Imp.	Start, UT	Max., UT
Feb. 14, 1956	0540	0553	2 720	66				N21 E32	2+	0538	0557
Feb. 23, 1956	0334	0336	18 000	448	0400	B	1.0×10^9	N23 W80	3	0331	
Mar. 8, 1956	0320	0322	421	5				No flare patrol			
Mar. 10, 1956	0447	0518	1 000	118	0900	B	1.1×10^8	N16 E88	2	0515	
Mar. 17, 1956	0002	0007	433	9				No logical flare association			
May 30, 1956	0234	0236	444	9				No logical flare association			
Nov. 17, 1956	0414	0424	117	11				S15 W75	1	0426	
Dec. 20, 1956	0444	0450	756	8				N12 E15	1	0432	
Dec. 29, 1956	0044	0056	1 117	26				N16 E59	1+	0040	0045
Jan. 5, 1957	0053	0056	228	6				No logical flare association			
Apr. 2, 1957	0301	0337	340	25				S16 W40	2	0309	
July 3, 1957	0727	0742	337	32	1000	B,L,H	2.0×10^7	N14 W40	3+	0712	0745
	0832	0843	763							0830	0840
Aug. 10, 1957	0126	0127	1 700	10				N26 W71	1	0125	0129
Aug. 30, 1957	2209	2214	619	6				No logical flare association			
Sep. 6, 1957	0753	0802	365	7				N27 W61	2	0755	0805
Sep. 7, 1957	0811	0813	2 015	12				N15 W88	1+	0810	0823
Sep. 11, 1957	0243	0304	373	27				N13 W02	3	0236	0300
Sep. 19, 1957	0359	0406	1 080	12				N23 E02	3	0350	0410
Oct. 23, 1957	0622	0623	1 640	10				S27 W77	1+	0621	
Nov. 22, 1957	0405	0410	380	8				N32 W26	2	0404	0409
Dec. 13, 1957	0155	0232	650	66				N15 E90	1	0227	0234
Dec. 26, 1957	0245	0246	2 650	16				No logical flare association			
Feb. 12, 1958		2345	125	8				S13 W56	1+	2334	
Feb. 26, 1958	0543	0552	500	9				S18 W61	2	0527	0550
Mar. 20, 1958	0636	0647	460	74				No logical flare association			
Apr. 2, 1958	0458	0500	840	6				S24 W34	1+	0502	
May 5, 1958	0412	0414	900	10				S18 W29	3	0356	0415
July 7, 1958	0027	0028	990	156	0330	B,L,H,K	2.5×10^8	N25 W08	3+	0020	0110
	0102	0111	1 700								

[a]List of PCA observers: B = Bailey; L = Leinbach; K = Kiruna; and H = Hakura & Goh

TABLE IV.- COMPILATION OF NAGOYA (3750 Mc/sec) RF BURST PARAMETERS AND ASSOCIATED SOLAR AND TERRESTIAL PHENOMENA FOR THE PERIOD 1956 TO 1961 - Continued

Date	RF burst, UT		RF peak intensity, 10^{-22} W/m^2-cps	RF burst energy above 10 percent of peak, 10^{-18} J/m^2-cps	Particle onset time, UT	PCA observers (a)	Particle event size, P > 30 MeV	Flare-			
	Start	Max.						Location	Imp.	Start, UT	Max., UT
July 29, 1958	0258	0304	2 000	15	0450	L		S14 W44	3	0259	0304
Aug. 16, 1958	0433	0439	5 800	300	0600	B,L,H,K	4.0×10^7	S14 W50	3+	0433	0440
Aug. 18, 1958	0805	0815	220	7				N20 E50	2	0805	0820
Aug. 26, 1958	0005	0041	5 050	550	0330	B,L,H,K	1.1×10^8	N20 W34	3	0005	0027
Aug. 20, 1958	0042	0043	1 450	15				N16 E18	2+	0042	0045
Sep. 22, 1958	0739		Sunset		1400	B,L,H	6.0×10^6	S19 W42	2+	0738	0750
Oct. 21, 1958	2323	2327	1 150	155				S04 W22	2+	2318	2330
Dec. 11, 1958	2350	2354	175	6				S03 W05	1	2355	2406
Dec. 23, 1958	0534	0605	1 020	54				S15 E66	2+	0545	0624
Feb. 1, 1959	0408	0422	550	6				N12 E83	3	0352	0423
Feb. 12, 1959	2250	2313	440	30	0800	B		N13 E48	3	2301	2325
Mar. 14, 1959	0017	0032	41	11				N23 E56	1+	0023	0051
Mar. 29, 1959	0746	0750	1 050	15				N17 E37	2	0747	0754
Apr. 5, 1959	2318	2323	2 300	37				N16 W67	3+	2316	2327
May 8, 1959	2255	2257	2 850	31				N21 E83	2+	2252	2257
May 10, 1959	>2200		Sunrise		0030(5/11)	B,L,K	9.6×10^8	N18 E47	3+	2102	2140
May 13, 1959	0510	0513	570	5				N21 E24	2+	0509	0515
May 17, 1959	0143	0149	175	7				N20 W26	1-	0104	0110
May 17, 1959	0523	0525	3 300	29				N20 W30	2+	0523	0527
May 17, 1959	0705	0707	1 280	10				N21 W30	1	0700	0708
May 18, 1959	0403	0404	1 750	16				No logical flare association			
May 26, 1959	2347	2350	360	10				N02 W14	1+	2348	2352
June 10, 1959	0245	0247	2 250	25				No logical flare association			
June 16, 1959	0623	0626	1 100	16				N16 E15	3	0618	0628
July 10, 1959	0200	0224	6 300	515	0700	B,L,K	1.0×10^9	N20 E50	3+	0206	0230
July 14, 1959	0330	0356	6 000	400	0730	B,L,K	1.3×10^9	N17 E04	3+	0325	0349
July 16, 1959			Sunrise		0000(7/17)	B,L,K	9.1×10^8	N16 W31	3+	2114	2132
Aug. 16, 1959	0740	0748	90	15				N15 W18	1+	0709	0716
Aug. 28, 1959	0024	0118	890	86				N11 E71	1	0027	0029 0113
Nov. 30, 1959	0247	0252	1 750	41				N08 E16	2+	0247	0250
Dec. 21, 1959	0043	0050	335	13.5				S05 W55	2	0045	0055

[a]List of PCA observers: B = Bailey; L = Leinbach; K = Kiruna; and H = Hakura & Goh

TABLE IV.- COMPILATION OF NAGOYA (3750 Mc/sec) RF BURST PARAMETERS AND ASSOCIATED SOLAR AND TERRESTIAL PHENOMENA FOR THE PERIOD 1956 TO 1961 - Concluded

Date	RF burst, UT		RF peak intensity, 10^{-22} w/m^2-cps	RF burst energy above 10 percent of peak, 10^{-18} J/m^2-cps	Particle onset time, UT	PCA observers (a)	Particle event size, P > 30 MeV	Flare-			
	Start	Max.						Location	Imp.	Start, UT	Max., UT
Feb. 18, 1960	0053	0101	765	29				S21 E90	1-	0122	0125
Feb. 20, 1960	0214	0227	190	9				S20 E63	2	0235	0238
Mar. 29, 1960	0655	0734	8 250	915	0800	B,G		N12 E30	2+	0650	0710
Apr. 3, 1960	0522	0524	395	6				N10 W35	2	0547	0548
Apr. 5, 1960	0140	0202	6 000	510	0700	B,L,K,G,VA	1.1×10^6	N12 W63	2	0215	0245
Apr. 28, 1960	0116	0130	260	17	0230	B,L,K,G,VA	5.0×10^6	S05 E34	3	0130	0137
Apr. 29, 1960	0139	0140	115	51	0500	B,L,G,VA	7.0×10^6	N14 W21	2+	0170	0210
	0356	0400	365								0400
May 13, 1960	0517	0532	3 750	500	0730	B,L,G,VA	4.0×10^6	N30 W67	3	0519	0532
June 10, 1960	0500	0510	300	5				N31 W62	2	0506	0518
June 27, 1960	0005	0012	50	7				S07 E35	3	0002	0023
June 27, 1960	?	0422	400	7				N20 W19	1+	0418	0430
June 29, 1960	0135	0148	840	23				N20 W50	1	0125	0148
Aug. 7, 1960	0725	0729	610	17				N19 E84	1	0724	0745
Aug. 11, 1960	0222	0253	610	11				N21 E35	2	0233	0255
Aug. 14, 1960	0514	0518	1 410	14				N22 W06	2+	0511	0525
Sep. 3, 1960	0039	0105	12 000	160	0500	B,L,G,VA	3.5×10^7	N18 E88	2+	0037	0108
Sep. 4, 1960	0010	0028	280	8				N17 W90	1-	2348	0017
Sep. 19, 1960	0659	0703	320	7				S18 E76	2	0659	0708
Sep. 26, 1960	0525	0539	1 680	108	1328	F,G	2.0×10^6	S22 W64	1+	0525	0537
Oct. 10, 1960	0708	0719	510	13				S17 W23	1+	0713	0722
Oct. 11, 1960	0520	0529	1 500	51	05--	G		S17 W36	2	0517	0535
Nov. 11, 1960	0315	0345	3 450	237	04--	G		N28 E12	2	0305	0340
Nov. 14, 1960	0258	0355	4 300	663	22-- ?	G		N27 W20	2+	0246	0304
Nov. 15, 1960	0219	0222	11 600	780	0430	B,L,G,VA	7.2×10^8	N25 W35	3	0207	0221
July 17, 1961	0718	0759	125	30				S07 W45	2	0721	0736
July 28, 1961	0226	0235	400	9				N12 W38	2	0240	0248
Sep. 15, 1961	0030	0040	280	3				S15 W11	1+	0031	0041
Sep. 28, 1961	2212	2217	1 690	48	2330	B,L,N	6.0×10^6	N13 E29	3	2202	2223

[a]List of PCA observers: B = Bailey; L = Leinbach; G = Gregory; VA = Van Allen, F = Fichtel; and N = NASA.

TABLE V.- OPTICAL DATA ASSOCIATED WITH PARTICLE EVENTS OCCURRING DURING THE PERIOD 1956 TO 1961

Date	Particle flux	Plage area	Plage brightness	Sunspot zurich mag. type class.	Sunspot area	Clustering of plages	Flare size	Flare location
10^9								
Feb. 23, 1956	1.0×10^9	16 000	3.5	F,E γ	1734 - 1437	Yes	3	N23 W80
July 10, 1959	1.0×10^9	11 000	3.0	H γ	1981 - 1412		3+	N20 E60
July 14, 1959	1.3×10^9	12 000	3.0	H γ	1981 - 1412		3+	N17 E04
Nov. 12, 1960	1.3×10^9	8 000	4.0	F β_γ	1775	No	3+	N27 W04
10^8								
Aug. 29, 1957	1.2×10^8	8 000	3.5	E γ	774	No	3	S31 E33
Jan. 20, 1957	2.0×10^8	9 000	3.0	H β_P	557	No	3	S30 W18
Mar. 23, 1958	2.5×10^8	15 000	3.5	E β_P	1539 - 1269		3+	S14 E78
July 7, 1958	2.5×10^8	6 200	3.0	E β_P	686	Yes	3+	N25 W08
Aug. 26, 1958	1.1×10^8	9 000	3.5	E β_γ and β_P	766	Yes	3	N20 W54
May 10, 1959	9.6×10^8	19 000	3.5	E β_γ	1552 - 947	No	3+	N18 E47
July 16, 1959	9.1×10^8	12 000	3.5	H γ	1981 - 1412	No	3+	N16 W30
July 18, 1961	3.0×10^8	5 700	3.5	E β_γ	1400	No	3+	S07 W59
Nov. 15, 1960	7.2×10^8	8 000	3.5	F β_γ	1775	No	3	N25 W35
10^7								
Aug. 31, 1956	2.5×10^7	7 800	4.0	E γ	837	No	3	N15 E16
July 3, 1957	2.0×10^7	7 000	3.5	H γ	500	No	3+	N10 W42
Oct. 20, 1957	5.0×10^7	14 200	3.5	F β_P	2373	No	3+	S26 W35
Aug. 16, 1958	4.0×10^7	10 000	3.5	G β_γ	935	Yes	3+	S14 W50
Aug. 22, 1958	7.0×10^7	6 400	3.5	E β_γ	1192	No	3	N18 W10
Sep. 3, 1960	3.5×10^7	10 000	3.5		800	No	2+	N18 E88
Feb. 9, 1958	1.1×10^7	18 000	4.0	D β_P	808 - 587	Yes	2+	S12 W14
Nov. 20, 1960	4.5×10^7	8 000	3.5	F β_γ	1775	No	2	N25 W90
July 12, 1961	4.0×10^7	5 700	3.5	E β_γ	1400	Yes	3	S07 E23
10^6								
Aug. 9, 1957	1.5×10^6	6 200	3.5	E γ	1092 - 845	No	1	S33 W77
Sep. 21, 1957	1.5×10^6	5 500	4.0	E β_γ	491	Yes	3	N10 W06
Sep. 22, 1958	6.0×10^6	15 000	3.5	E β_P	1087	Yes	2	S19 W42
Aug. 18, 1959	1.8×10^6	6 800	3.5	E γ and β_P	1119 - 745	Yes	3+	N12 W33
Apr. 1, 1960	5.0×10^6	3 000	3.0	F β_γ	1650	No	3	N12 W11

TABLE V.- OPTICAL DATA ASSOCIATED WITH PARTICLE EVENTS OCCURRING DURING THE PERIOD 1956 TO 1961 - Concluded

Date	Particle flux	Plage area	Plage brightness	Sunspot zurich mag. type class.	Sunspot area	Clustering of plages	Flare size	Flare location
10^6								
Apr. 5, 1960	1.1×10^6		3.0	F γ	1650	No	2	N12 W63
Apr. 28, 1960	5.0×10^6	5 000	3.0	β_p	<500	No	3	S05 E34
Apr. 29, 1960	7.0×10^6	4 000	3.0	H γ	850		2+	N14 W21
May 4, 1960	6.0×10^6	4 500	2.5	α	850	No	3	N13 W90
May 6, 1960	4.0×10^6	3 900	4.0	β_p	<500	No	3+	S09 E07
May 13, 1960	4.0×10^6	4 000		F γ	1800	No	3	N29 W67
Aug. 26, 1960	2.0×10^6	3 000	3.0		925	No	1+	S22 W64
July 11, 1961	3.0×10^6	4 000	4.0	E β_γ	1400		3	S07 E32
July 20, 1961	5.0×10^6	5 600	3.5	E β_γ	1400		3	S07 W90
Sep. 28, 1961	6.0×10^6	3 600	3.0	β_F	<500		3	N13 E29
10^5								
June 13, 1959	8.5×10^5	9 000	3.5	γ	1111 - 856	Yes	1	N17 E58
Jan. 11, 1960	4.0×10^5	3 500	2.5	H α_p	575	No	3	N22 E03
June 1, 1960	4.0×10^5	8 000	3.5	β_p	<500	No	3+	N29 E46
Aug. 11, 1960	6.0×10^5	13 000	3.5	J β_α	1100	No	2+	N22 E26

TABLE VI.- OPTICAL AND RF PARAMETERS USED IN THE COMBINED FALSE ALARM STUDY FOR 3750 Mc/sec RF BURSTS

Date	Plage area	Plage brightness	Sunspot area	Flare size	Flare location	RF burst energy, 10^{-18} W/m^2-cps	Predicted event size RF criteria	Predicted event size span criteria	Actual event size
Feb. 14, 1956	[a]8 000	3.0	1563	2+	N21 E32	66	10^7	10^7	
Feb. 23, 1956	[a]16 000	3.5	1734 - 1437	3	N23 W80	448	10^9	10^9	1.0×10^9
Mar. 8, 1956	No flare patrol					5	10^5	?	
Mar. 10, 1956	6 000	3.0	-	2	N16 E88	118	10^8	10^5	No estimate
Mar. 17, 1956	No logical flare association					9	10^6	No event	
May 30, 1956	No logical flare association					9	10^6	No event	
Nov. 17, 1956	[a]8 000	3.0	1866 - 1407	1	S15 W75	11	10^6	10^6	
Dec. 20, 1956	5 400	3.5	1498 - 977	1	N12 E15	8	10^6	No event	
Dec. 29, 1956	5 500	4.0	2089 - 1351	1+	N16 E59	26	10^7	10^5	
Jan. 5, 1957	No logical flare association					6	10^6	No event	
Apr. 2, 1957	4 500	3.5	734 - 240	2	S16 W40	25	10^7	10^6	
July 3, 1957	7 000	3.5	606 - 537	3+	N14 W40	32	10^7	10^7	2.0×10^7
Aug. 10, 1957	5 000	3.5	775 - 629	1	N26 W71	10	10^6	10^6	
Aug. 30, 1957	No logical flare association					6	10^6	No event	
Sep. 6, 1957	17 000	3.0	740 - 348 987 - 459	2	N27 W61	7	10^6	No event	
Sep. 7, 1957	17 000	3.5	740 - 348	1+	N15 W88	12	10^6	10^6	
Sep. 11, 1957	8 000	4.0	664	3	N13 W02	27	10^7	10^7	
Sep. 19, 1957	[a]8 000	4.0	2122	3	N23 E02	12	10^6	10^6	
Oct. 23, 1957	21 000	4.0	2480 - 2074	1+	S27 W77	10	10^6	10^6	
Nov. 22, 1957	7 000	4.0	706 - 381	2	N23 W26	8	10^6	No event	
Dec. 13, 1957	7 000	4.0	1434 - 939	1	N15 E90	66	10^7	10^5	
Dec. 26, 1957	No logical flare association					16	10^6	No event	
Feb. 12, 1958	Not available			1+	S13 W56	8	10^6	No event	
Feb. 26, 1958	[a]3 500	2.5	646 - 460	2	S18 W61	9	10^6	10^6	
Mar. 20, 1958	No logical flare association					74	10^7	No event	
Apr. 2, 1958	[a]6 000	3.0	1992 - 1325	1+	S24 W34	6	10^6	No event	
May 5, 1958	10 000	3.0	2060 - 1332	3	S18 W29	10	10^6	10^6	
July 7, 1958	[a]6 200	3.0	686	3+	N25 W08	156	10^8	10^8	2.5×10^8
July 29, 1958	20 000	3.0	682 - 364	3	S14 W44	15	10^6	10^6	No estimate
Aug. 16, 1958	[a]10 000	3.5	1150 - 876	3+	S14 W50	300	10^9	10^8	4.0×10^7
Aug. 18, 1958	3 600	4.0	1463 - 1072	2	N20 E50	7	10^6	No event	
Aug. 20, 1958	6 500	3.5	1463 - 1072	2+	N16 E18	15	10^6	10^5	

[a]Complex grouping of plage regions; area given is for plage region associated with event.

TABLE VI.- OPTICAL AND RF PARAMETERS USED IN THE COMBINED FALSE ALARM STUDY FOR 3750 Mc/sec RF BURSTS - Continued

Date	Plage area	Plage brightness	Sunspot area	Flare size	Flare location	RF burst energy 10^{-18} W/m^2-cps	Predicted event size RF criteria	Predicted event size span criteria	Actual event size
Aug. 26, 1958	[a]9 000	3.5	1463 - 1072	3	N20 W54	550	10^9	10^8	1.1×10^8
Sep. 22, 1958	15 000	3.5	1824 - 1289	2+	S19 W42	Sunset	-	-	6.0×10^6
Oct. 21, 1958	4 500	3.5	872	2+	S04 W22	155	10^8	10^7	
Dec. 11, 1958	8 500	3.0	1318 - 710	1	S03 W05	6	10^6	No event	
Dec. 23, 1958	9 000	3.5	1608	2+	S15 E66	54	10^7	10^7	
Feb. 1, 1959	13 000	3.0	590	3	N12 E83	6	10^6	No event	
Feb. 12, 1959	6 300	3.0	1064 - 866	3	N13 E48	30	10^7	10^7	No estimate
Mar. 14, 1959	[a]11 000	3.0	2274 - 1732	1+	N23 E56	11	10^6	10^5	
Mar. 29, 1959	12 000	3.5	746 - 490	2	N17 E37	15	10^6	10^5	
Apr. 5, 1959	[a]10 000	3.0	746 - 490	3+	N16 W67	37	10^7	10^6	
May 8, 1959	11 000	3.5	1552 - 947	2+	N21 E83	31	10^7	10^7	
May 10, 1959	19 000	3.5	1552 - 947	3+	N18 E47	Sunrise	-	-	9.6×10^8
May 13, 1959	17 000	3.5	1552 - 947	2+	N21 E24	5	10^5	No event	
May 17, 1959	[a]17 000	3.5	1552 - 947	1-	N20 W26	7	10^6	No event	
May 17, 1959	[a]17 000	3.5	1552 - 947	2+	N20 W30	29	10^7	10^7	
May 17, 1959	[a]17 000	3.5	1552 - 947	1	N21 W30	10	10^6	10^6	
May 18, 1959	No logical flare association					16	10^6	No event	
May 26, 1959	[a]2 100	3.5	772 - 399	1+	N02 W14	10	10^6	10^5	
June 10, 1959	No logical flare association					25	10^7	No event	
June 16, 1959	9 000	3.5	1111 - 856	3	N16 E15	16	10^6	10^6	
July 10, 1959	11 000	3.0	1981 - 1412	3+	N20 E60	515	10^9	10^9	1.0×10^9
July 14, 1959	12 000	3.0	1981 - 1412	3+	N17 E04	400	10^9	10^9	1.3×10^9
July 16, 1959	12 000	3.5	1981 - 1412	3+	N16 W31	Sunrise	-	-	9.1×10^8
Aug. 16, 1959	6 000	2.5	1119 - 745	1+	N15 W78	15	10^6	10^6	
Aug. 28, 1959	[a]3 000	2.5	1011 - 536 670 - 339	1	N11 E71	86	10^8	10^5	
Nov. 30, 1959	8 500	3.5	2622 - 1948	2+	N08 E16	41	10^7	10^7	
Dec. 21, 1959	[a]2 600	3.0	-	2	S05 W55	13.5	10^6	10^5	
Feb. 18, 1960	1 200	3.5	-	1-	S21 E90	29	10^7	No event	
Feb. 20, 1960	1 200	3.5	-	2	S20 E63	9	10^6	No event	
Mar. 29, 1960	3 000	3.5	1650	2+	N12 E30	915	10^9	10^5	No estimate
Apr. 3, 1960	3 500	3.0	1650	2	N10 W35	6	10^6	No event	

[a]Complex grouping of plage regions; area given is for plage region associated with event.

TABLE VI.- OPTICAL AND RF PARAMETERS USED IN THE COMBINED FALSE ALARM STUDY FOR 3750 Mc/sec RF BURSTS - Concluded

Date	Plage area	Plage brightness	Sunspot area	Flare size	Flare location	RF burst energy 10^{-18} w/m^2-cps	Predicted event size RF criteria	Predicted event size span criteria	Actual event size
Apr. 5, 1960	3 500	3.0	1650	2	N12 W63	510	10^9	10^6	1.1×10^6
Apr. 28, 1960	5 000	3.0	<500	3	S05 E34	17	10^6	10^6	5.0×10^6
Apr. 29, 1960	4 000	3.0	850	2+	N14 W21	51	10^7	10^7	7.0×10^6
May 13, 1960	4 000	3.0	1800	3	N30 W67	500	10^9	10^7	4.0×10^6
June 10, 1960	6 000	3.0	-	2	N31 W62	5	10^5	No event	
June 27, 1960	6 000	3.0	-	3	S07 E35	7	10^6	No event	
June 27, 1960	3 700	3.0	-	1+	N20 W19	7	10^6	No event	
June 29, 1960	2 200	3.0	-	1	N20 W50	23	10^7	10^5	
Aug. 7, 1960	6 500	3.5	1100	1	N19 E84	17	10^6	10^5	
Aug. 11, 1960	13 000	3.5	1100	2	N21 E35	11	10^6	10^5	
Aug. 14, 1960	11 000	3.5	1100	2+	N22 W06	14	10^6	10^6	
Sep. 3, 1960	10 000	3.5	800	2+	N18 E88	160	10^8	10^7	3.5×10^7
Sep. 4, 1960	Data not available			1-	N17 W90	8	10^6	No event	
Sep. 19, 1960	6 000	3.0	-	2	S18 E76	7	10^6	No event	
Sep. 26, 1960	5 600	3.0	925	1+	S22 W64	108	10^8	10^6	2.0×10^6
Oct. 10, 1960	4 400	3.0	-	1+	S17 W23	13	10^6	10^6	
Oct. 11, 1960	4 000	3.0	<500	2	S17 W36	51	10^7	10^6	No estimate
Nov. 11, 1960	9 100	3.5	1775	2	N28 E12	237	10^8	10^5	No estimate
Nov. 14, 1960	8 000	3.5	1775	2+	N27 W20	663	10^9	10^7	No estimate
Nov. 15, 1960	8 000	3.5	1775	3	N25 W35	780	10^9	10^9	7.2×10^8
July 17, 1961	5 600	3.5	1400	2	S07 W45	30	10^7	10^6	
July 28, 1961	4 000	3.5	725	2	N12 W38	9	10^6	No event	
Sep. 15, 1961	[a]6 800	3.0	950	1+	S15 W11	3	10^5	No event	
Sep. 28, 1961	3 600	3.0	<500	3	N13 E29	48	10^7	10^6	6.0×10^6

[a]Complex grouping of plage regions, area given is for plage region associated with event.

TABLE VII.- OPTICAL AND RF PARAMETERS USED IN THE COMBINED FALSE ALARM STUDY FOR 2800 Mc/sec RF BURSTS

Date	Plage area	Plage brightness	Sunspot area	Flare imp.	Flare location	RF burst energy, 10^{-18} w/m^2-cps	Predicted event size RF criteria	Predicted event size span criteria	Actual event size
June 18, 1955	6 000	4.0	639	3	S22 W21	43	10^7	10^7	
July 9, 1955	No flare data available					30	10^6	?	
Feb. 16, 1956	[a]8 000	4.0	1734 - 1437	2	N20 E08	60	10^7	10^5	
Feb. 19, 1956	[a]18 000	3.5	1734 - 1437	1+	N25 W23	29	10^6	10^6	
Mar. 13, 1956	10 000	3.5	1237	2	N21 E50	14	10^6	10^5	
Mar. 15, 1956	[a]9 000	3.0	1089	2	N22 E21	43	10^7	10^5	
June 20, 1956	No flare data available					12	10^6	?	
Sep. 17, 1956	[a]17 500	3.5	361	2+	S20 W17	13	10^6	10^6	
Nov. 13, 1956	4 000	3.5	814 - 465	2	N16 W10	13	10^6	10^6	No estimate
Dec. 26, 1956	3 000	3.5	1002	2	S17 W11	132	10^7	10^6	
Jan. 6, 1957	5 000	3.5	2089 - 1351	1-	N16 W55	42	10^7	No event	
Apr. 12, 1957	5 100	3.0	369 - 237	2	S25 W73	12	10^6	No event	
Apr. 14, 1957	6 000	3.5	937 - 665	1	S23 W28	40	10^7	10^6	
Apr. 16, 1957	9 000	3.0	1000 - 432	3	N30 E85	87	10^7	10^7	
Apr. 17, 1957	9 000	3.0	1000 - 432	3+	N20 E69	546	10^9	10^8	
June 3, 1957	4 500	3.0	787	3	S18 W18	17	10^6	10^6	
June 19, 1957	9 000	3.5	931	2	N20 E45	34	10^6	10^5	No estimate
July 15, 1957	No associable flare					12	10^6	No event	
July 16, 1957	1 200	2.5	769 - 530	1+	S33 W28	23	10^6	No event	
July 20, 1957	No associable flare					14	10^6	No event	
July 24, 1957	5 500	3.0	504	3	S24 W27	94	10^7	10^7	No estimate
Aug. 1, 1957	6 500	3.5	1092 - 845	1	S35 E04	22	10^6	10^5	
Aug. 9, 1957	6 200	3.5	1092 - 845	1	S33 W77	27	10^6	10^6	1.5×10^6
Aug. 28, 1957	8 200	3.0	774	2+	S28 E30	10	10^6	10^5	No estimate
Aug. 31, 1957	8 000	3.5	1317	3	N25 W02	350	10^8	10^8	No estimate
Sep. 2, 1957	6 000	3.5	626	2+	S34 W36	30	10^6	10^6	No estimate
Sep. 3, 1957	15 000	3.5	597	3	N23 W30	51	10^7	10^7	
Sep. 18, 1957	[a]6 800	4.5	1998	3+	N20 E02	47	10^7	10^7	
Sep. 21, 1957	5 500	4.0	491	3	N10 W06	13	10^6	10^6	1.5×10^6
Sep. 26, 1957	19 500	3.0	232	3	N22 E15	25	10^6	10^5	No estimate
Oct. 20, 1957	14 200	3.5	2373	3+	S26 W35	209	10^8	10^8	5.0×10^7
Jan. 15, 1958	9 000	3.5	786	2+	S13 W58	21	10^6	10^6	

[a]Complex grouping of plage regions; area given is for plage region associated with event.

TABLE VII.- OPTICAL AND RF PARAMETERS USED IN THE COMBINED FALSE ALARM STUDY FOR

2800 Mc/sec RF BURSTS - Continued

Date	Plage area	Plage brightness	Sunspot area	Flare imp.	Flare location	RF burst energy, 10^{-18} w/m^2-cps	Predicted event size RF criteria	Predicted event size spot criteria	Actual event size
June 5, 1958	4 000	3.0	314	2+	S18 E69	35	10^6	10^5	
June 28, 1958	12 000	3.0	245 - 114	1-	S26 W20	32	10^6	No event	
July 30, 1958	[a]19 000	3.0	1795 - 901	2	S13 W64	15	10^6	10^6	
Aug. 2, 1958	[a]19 000	3.0	1795 - 901	1-	S14 W90	26	10^6	No event	
Aug. 22, 1958	6 400	3.5	1192	3	N18 W10	192	10^8	10^8	7.0×10^7
Oct. 24, 1958	7 000	3.5	439	2+	S05 W57	18	10^6	10^6	
Dec. 11, 1958	8 500	3.0	1318 - 710	2	S02 E00	14	10^6	10^6	
Dec. 12, 1958	10 000	3.5	1318	2+	S03 W08	20	10^6	10^6	
Jan. 21, 1959	7 500	3.5	1886 - 1476	3	N10 E48	12	10^6	10^6	
Jan. 24, 1959	2 400 6 000	3.5 3.0	- -	1 1	S06 E20 N18 W21	12	10^6	10^5	
Jan. 25, 1959	[a]13 000	3.0	1400 - 945	2	N18 W50	50	10^7	10^6	
Feb. 9, 1959	4 000	3.0	1064 - 866	2+	N09 E87	10	10^6	10^5	
Mar. 22, 1959	8 500	4.0	2274 - 1732	1+	N29 W50	12	10^6	10^6	
Apr. 7, 1959	4 000	3.5	513 - 264	2	N10 E84	26	10^6	10^5	
May 8, 1959	11 000	3.5	1152 - 947 806 - 563	2+	N21 E83	29	10^6	10^5	
May 10, 1959	19 000	3.5	1552 - 947	3+	N18 E47	811	10^9	10^8	9.6×10^8
May 11, 1959	17 500	3.5	1152 - 947	3	N10 E41	75	10^7	10^7	
June 9, 1959	9 000	3.5	1111 - 856	2	N17 E90	146	10^8	10^5	
June 18, 1959	9 000	3.5	1111 - 856	3+	N16 W12	14	10^6	10^6	
July 9, 1959	12 000	3.5	1981 - 1412	2	N18 E67	15	10^6	10^5	
July 9, 1959	12 000	3.5	1981 - 1412	2	N19 E48	30	10^6	10^5	
July 16, 1959	12 000	3.5	1981 - 1412	3+	N16 W31	732	10^9	10^9	9.1×10^8
Aug. 31, 1959	7 500	3.0	1011 - 536	1+	W10 E11	10	10^6	10^5	
Dec. 2, 1959	9 000	3.5	2622 - 1948	2+	N07 W16	11	10^6	10^6	
Dec. 4, 1959	13 000	3.0	2622 - 1948	2+	N06 W44	16	10^6	10^6	
Jan. 11, 1960	3 500	2.5	575	3	N22 E03	13	10^6	10^6	4.0×10^5
Jan. 15, 1960	5 000	3.5	1150	2	S20 W68	117	10^7	10^6	No estimate
Mar. 28, 1960	3 000	3.5	1650	2	N14 E37	127	10^7	10^5	
Mar. 30, 1960	3 500	3.0	1650	2	N12 E11	160	10^8	10^5	No estimate
Apr. 3, 1960	No associable flare					18	10^6		
May 4, 1960	4 500	2.5	850	3	N13 W90	69	10^7	10^6	6.0×10^6
May 6, 1960	3 900	4.0	<500	3+	S09 E07	69	10^7	10^6	4.0×10^6

[a]Complex grouping of plage regions, area given is for plage region associated with event.

TABLE VII.- OPTICAL AND RF PARAMETERS USED IN THE COMBINED FALSE ALARM STUDY FOR

2800 Mc/sec RF BURSTS - Concluded

Date	Plage area	Plage brightness	Sunspot area	Flare imp.	Flare location	RF burst energy, 10^{-18} w/m^2-cps	Predicted event size RF criteria	Predicted event size span criteria	Actual event size
June 25, 1960	2 500	3.5	-	3	N21 E06	46	10^7	10^5	No estimate
June 27, 1960	2 500	3.5	-	3	N22 W27	17	10^6	10^5	No estimate
Aug. 11, 1960	13 000	3.5	1100	2+	N22 E26	26	10^6	10^5	6.0×10^5
Sep. 16, 1960	3 500	4.0	925	1	S22 E67	185	10^8	10^5	
Oct. 23, 1960	3 500	3.0	1225	1+	N22 E90	22	10^6	10^5	
Nov. 6, 1960	5 800	3.0	-	3	N13 E07	20	10^6	10^6	
Nov. 12, 1960	8 000	4.0	1775	3+	N27 W04	606	10^9	10^9	1.3×10^9
Dec. 5, 1960	7 500	3.5	-	3+	N26 E74	23	10^6	10^6	No estimate
July 11, 1961	4 000	4.0	1400	3	S07 E32	138	10^7	10^7	3.0×10^6
July 12, 1961	[a]5 700	3.5	1400	3	S07 E23	88	10^7	10^7	4.0×10^7
July 15, 1961	[a]5 700	3.5	1400	2	S07 W20	36	10^6	10^6	No estimate
July 20, 1961	5 600	3.5	1400	3	S06 W09	94	10^7	10^7	5.0×10^6
Sep. 10, 1961	6 000	3.5	1350	1	N08 W80	95	10^7	10^6	No estimate
Sep. 28, 1961	3 600	3.0	<500	3	N13 E29	36	10^6	10^6	6.0×10^6
Nov. 10, 1961	2 200	3.0	-	1+	N19 W90	8	No event	No event	No estimate

[a]Complex grouping of plage regions, area given is for plage region associated with event.

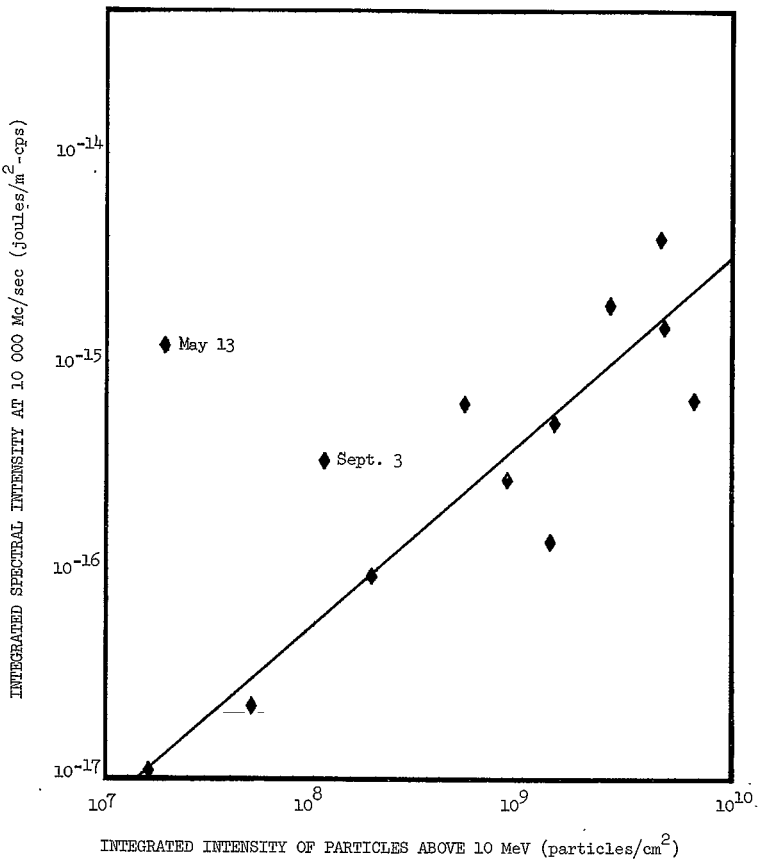

Figure 1.- Integrated radio emission at 10 000 Mc/sec versus integrated intensity of solar particles above 10 MeV at the earth for various events.

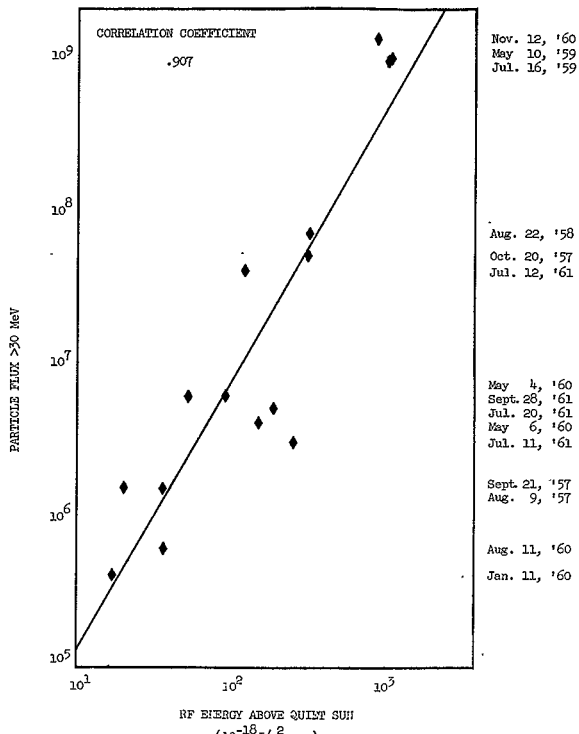

Figure 2.- Webber's integrated particle fluxes >30 MeV correlated with 2800 Mc/sec RF burst energies above quiet sun level.

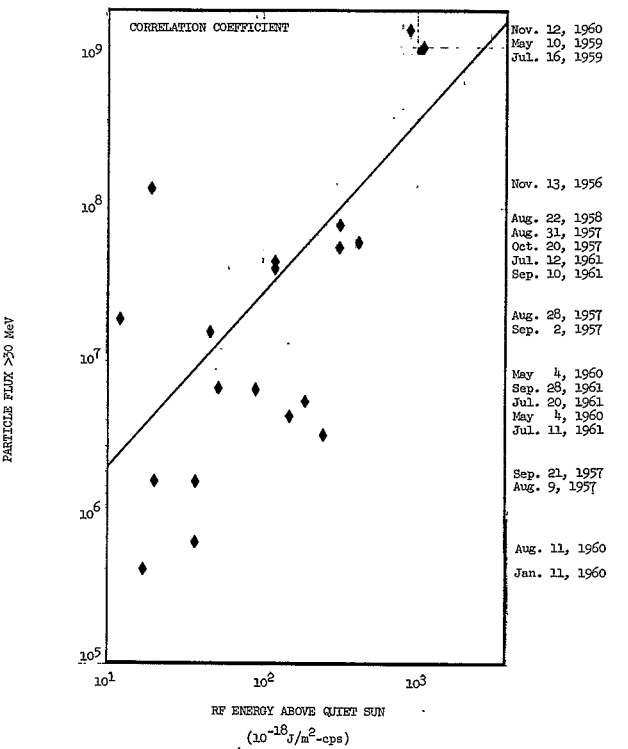

Figure 3.- Combination of Webber and forward scatter particle fluxes >50 MeV versus RF burst energies above the quiet sun.

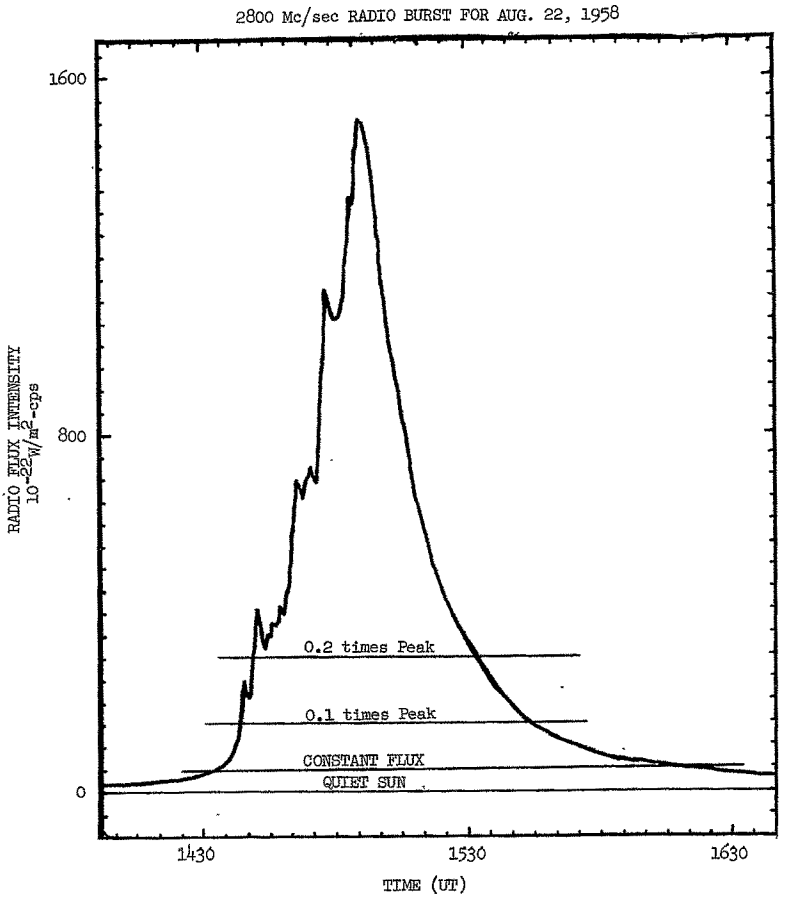

Figure 4.- Ottawa burst showing base lines for constant flux ($50 \times 10^{-22} W/m^2$-cps), 0.1 and 0.2 times peak intensity above which RF burst energies were determined for correlations.

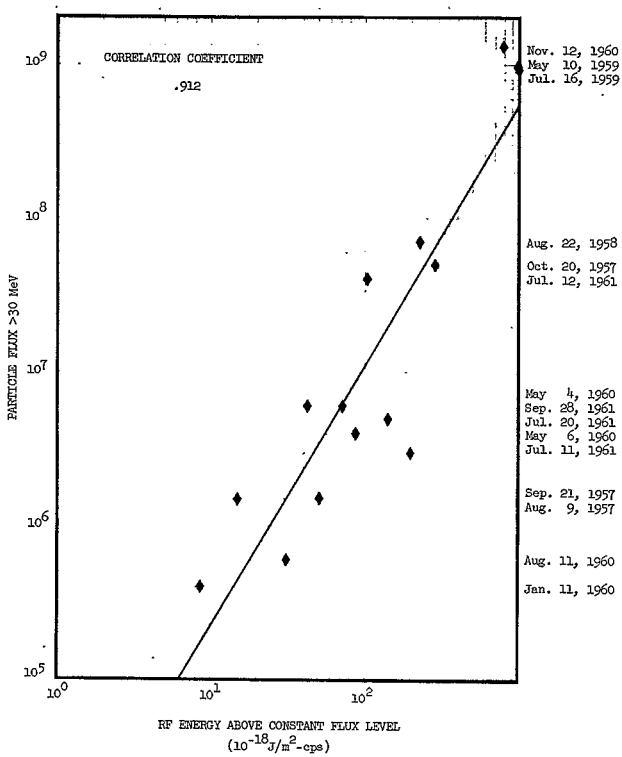

Figure 5.- Webber's integrated particle fluxes >30 MeV correlated with 2800 Mc/sec RF burst energies above a constant flux level of 50×10^{-22} W/m^2-cps.

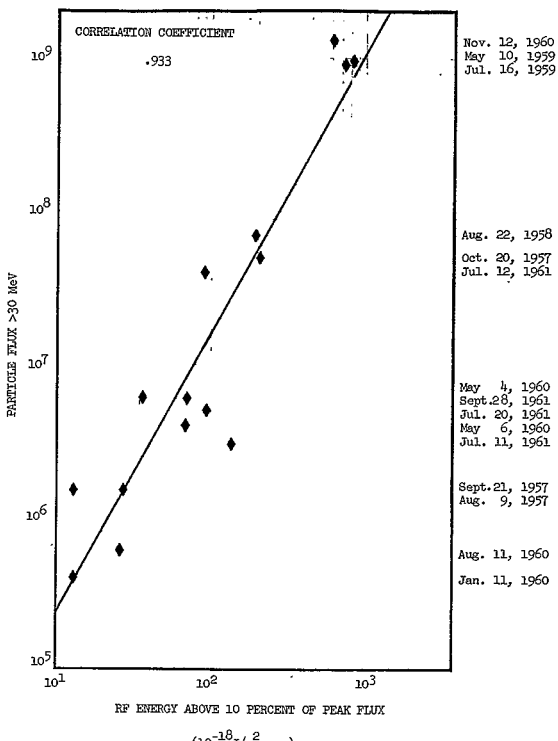

Figure 6.- Webber's integrated particle fluxes >30 MeV correlated with 2800 Mc/sec RF burst energies above a baseline of 10 percent of burst's peak flux intensity.

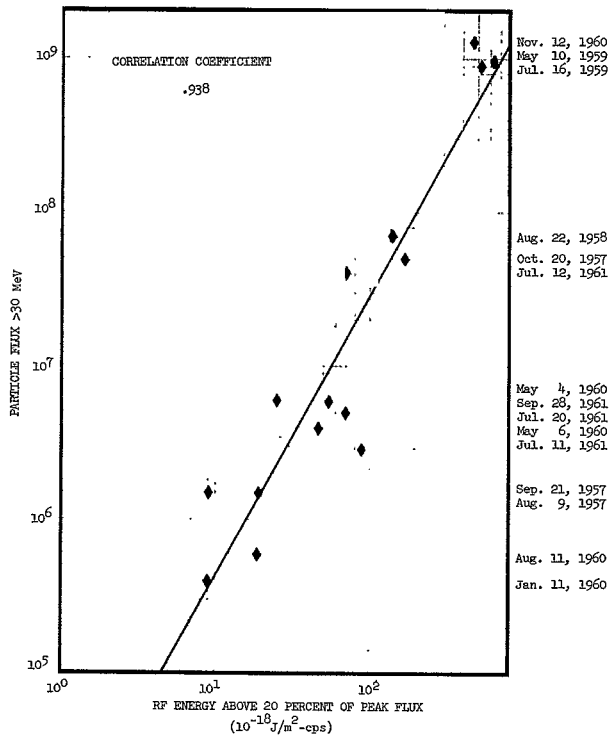

Figure 7.- Webber's integrated particle fluxes >30 MeV correlated with 2800 Mc/sec RF burst energies above a baseline of 20 percent of burst's peak flux intensity.

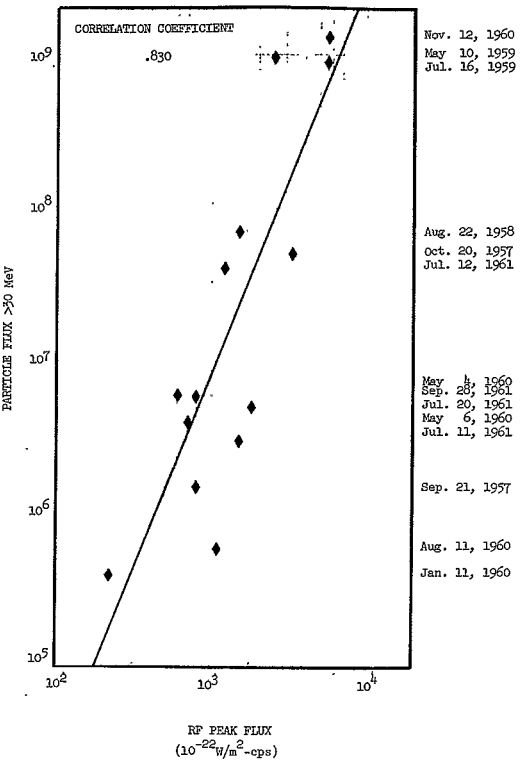

Figure 8.- Webber's particle fluxes >30 MeV versus associated 2800 Mc/sec RF burst peak fluxes.

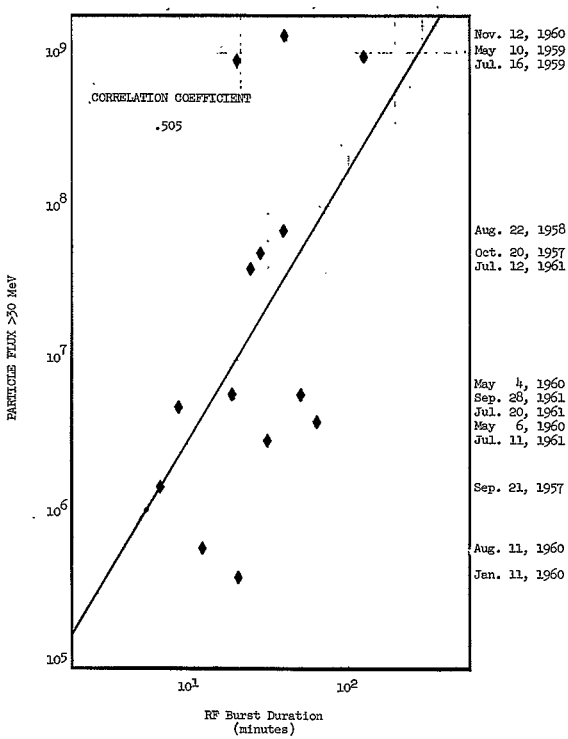

Figure 9.- Webber's particle fluxes >30 MeV versus duration of associated RF burst durations in minutes.

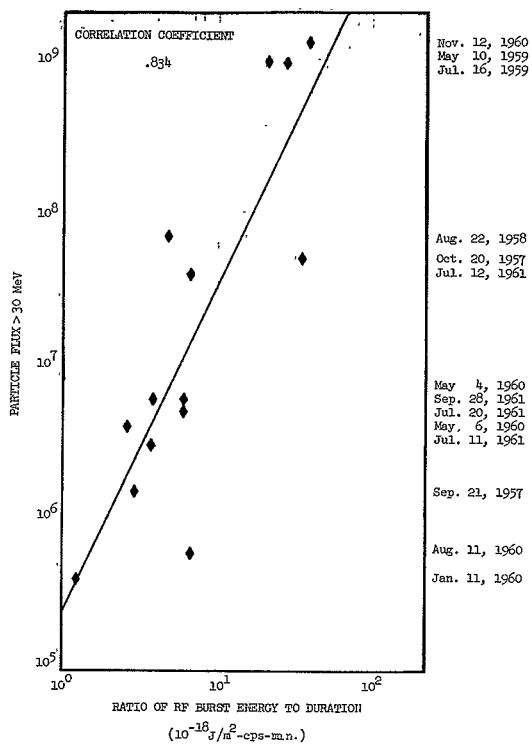

Figure 10.- Webber's integrated particle fluxes >30 MeV correlated with the ratio of RF burst energy above quiet sun to RF burst duration in minutes.

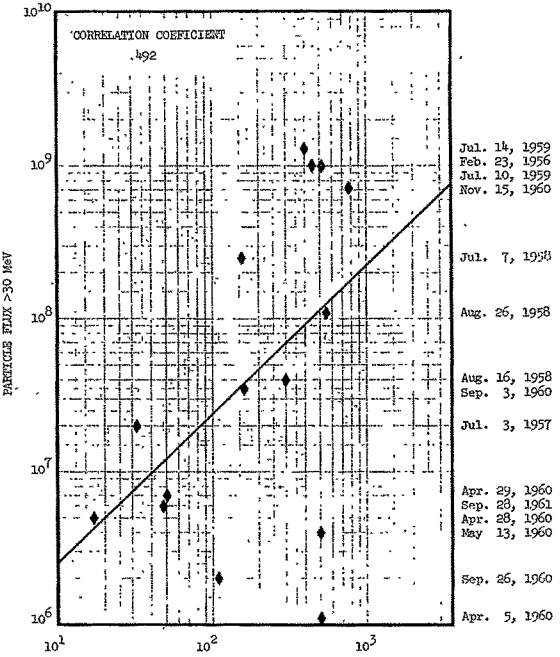

Figure 11.- Webber particle fluxes >30 MeV versus Nagoya (3750 Mc/sec) RF burst energies above 10 percent of peak flux.

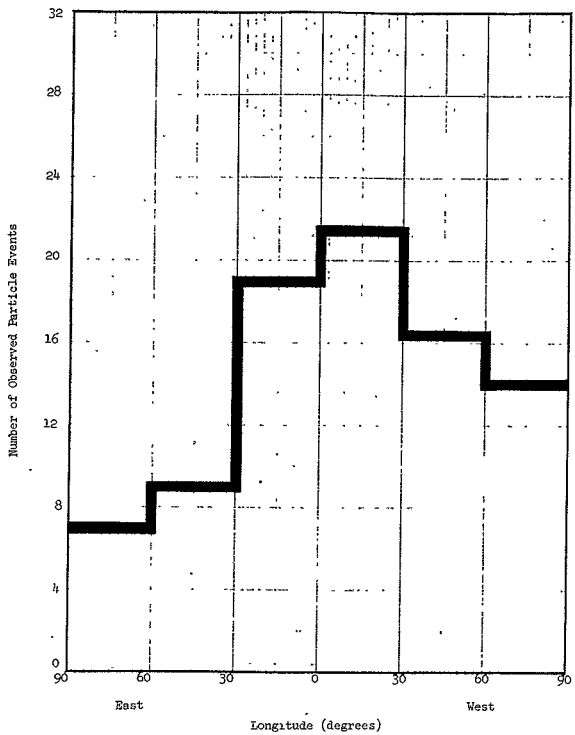

Figure 12.- Number of particle events versus heliographic position.

(Webber, Bailey, Gregory, Leinbach, Van Allen, Data)

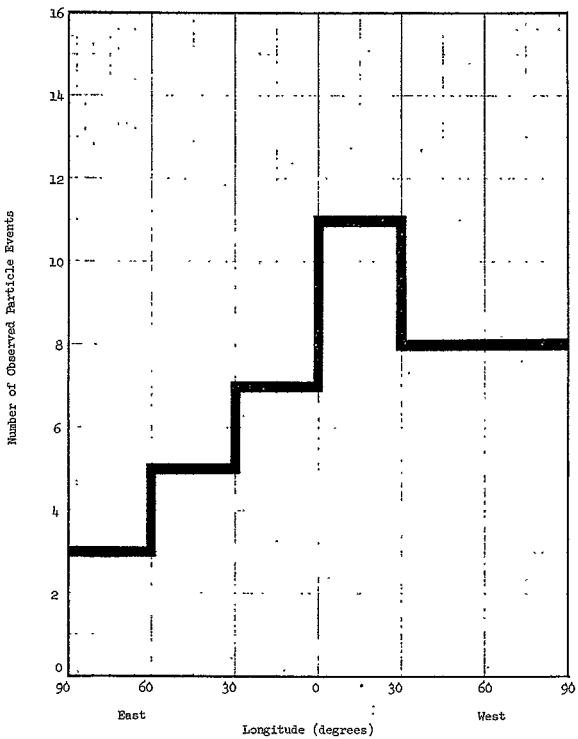

Figure 13.- Number of particle events versus heliographic position.

(Webber Data)

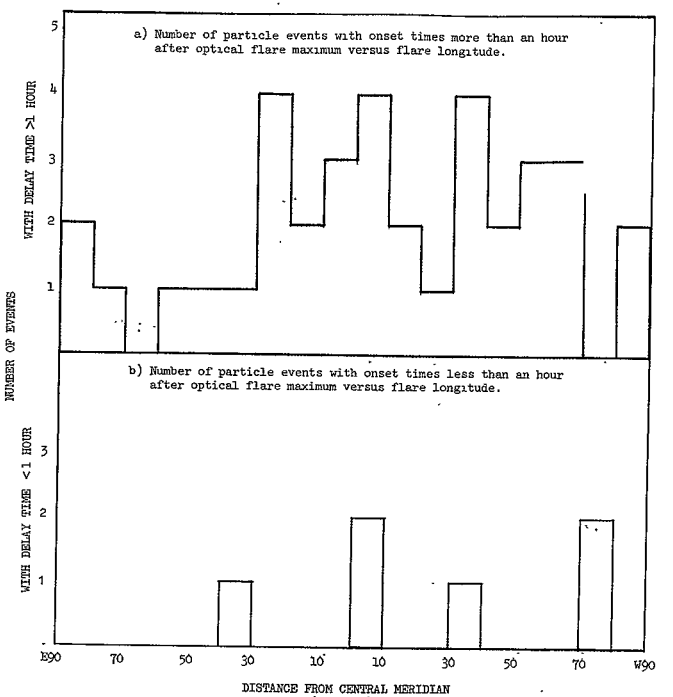

Figure 14.- Longitudinal distribution of PCA flares catergorized according to particle transit time. (<1 hour and >1 hour)

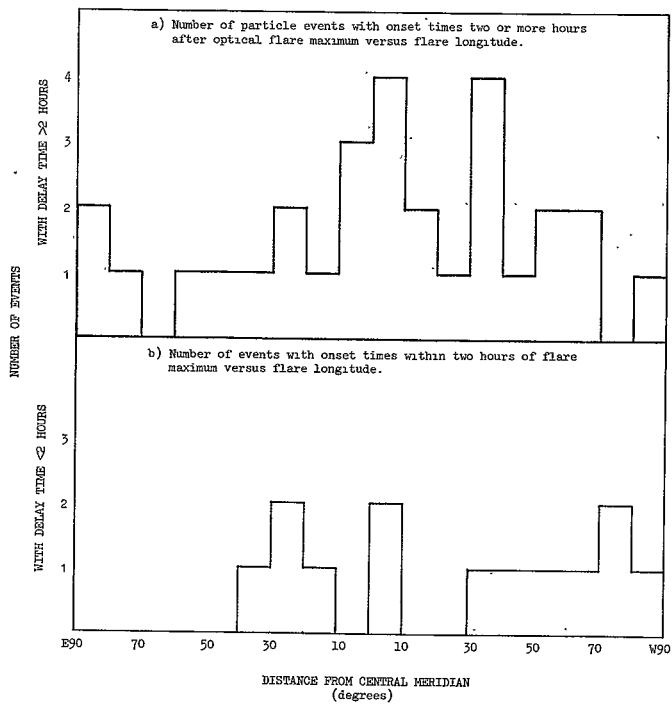

Figure 15.- Longitudinal distribution of PCA flares catergorized according to particle transit time. (<2 hours and >2 hours)

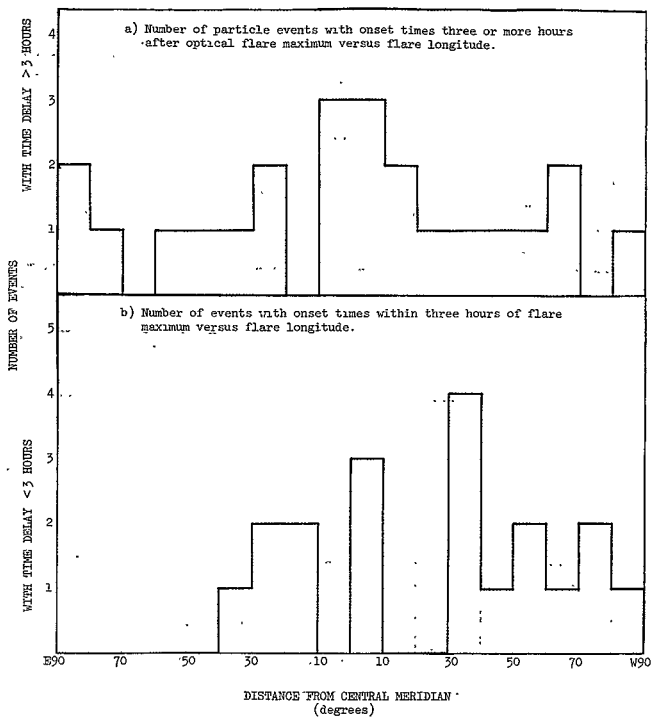

Figure 16.- Longitudinal distribution of PCA flares catergorized according to particle transit time. (<3 hours and >3 hours)

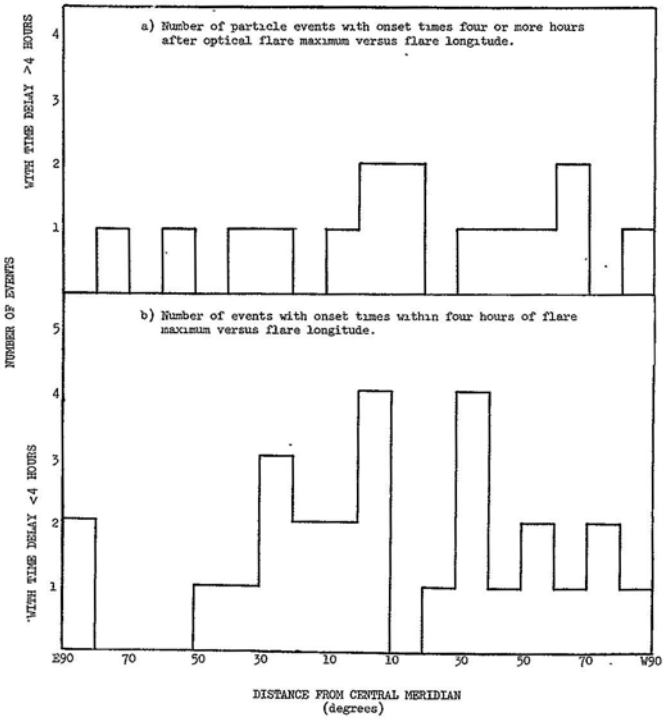

Figure 17.- Longitudinal distribution of PCA flares catergorized according to particle transit time. (<4 hours and >4 hours)

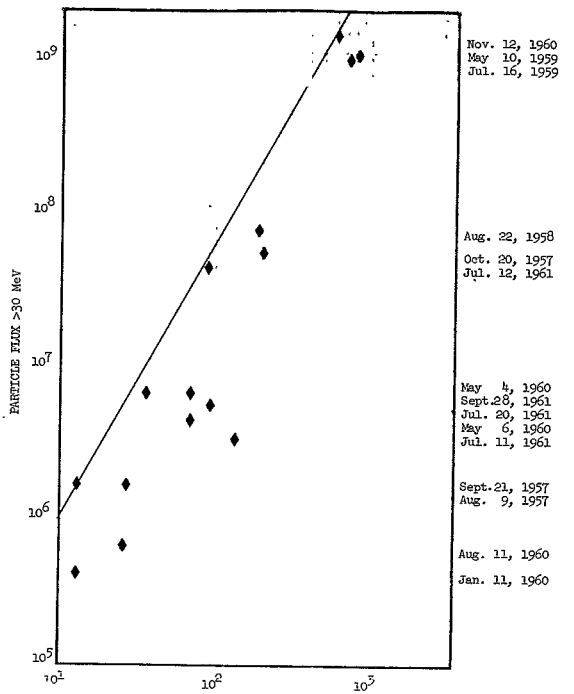

Figure 18.- Webber's integrated particle fluxes >30 MeV correlated with 2800 Mc/sec RF burst energies above a baseline of 10 percent of burst's peak flux intensity. The line drawn is an envelope curve and parallel to the least square fit used in figure 6.

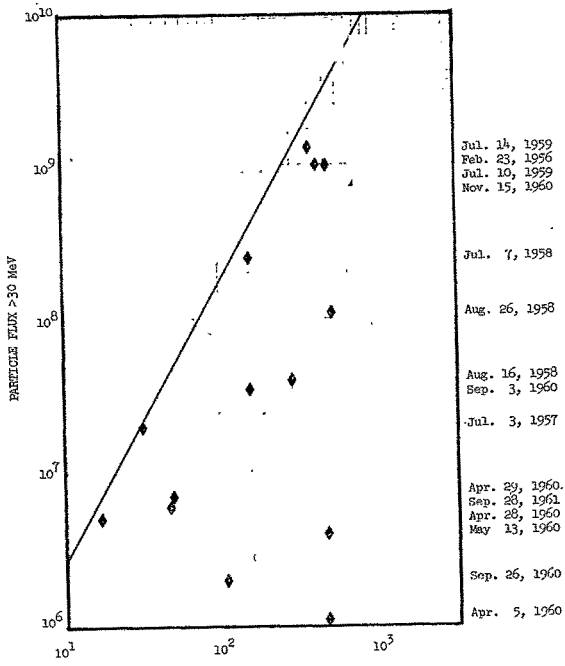

Figure 19.- Webber particle fluxes >30 MeV versus Nagoya (3750 Mc/sec) RF burst energies above 10 percent of peak flux shown with an envelope curve drawn parallel to the least square fit for Ottawa RF burst energies above 10 percent of peak flux (fig. 6).